Supporting Information

Spectroscopic and Electrochemical Studies of Tin(IV) Complexes with a Noninnocent N_2S_2 and N_2O_2 Ligands based on acenaphthene

*Liliya D. Labutskaya, Varvara A. Klok, Irina V. Krylova, Pavel G. Shangin, Mikhail E. Minyaev, Evgeny V. Tretyakov, Mikhail A. Syroeshkin, Mikhail P. Egorov, Elena N. Nikolaevskaya**

N. D. Zelinsky Institute of Organic Chemistry Russian Academy of Sciences

Table of content

S1. Instrumentation

^{1}H NMR (300 MHz) and ^{13}C NMR (75 MHz) spectra were recorded using a Bruker Avance-300, and 119Sn (112 MHz) – using a Bruker AM300 at ambient temperature. NMR spectra were referenced using the signal of a residual protio solvent (for ^{1}H NMR), the dominant solvent signal (for ^{13}C NMR), and the Me_4Sn signal (for ^{119}Sn NMR). High-resolution mass spectra (HRMS) were recorded using a Bruker micrOTOF II instrument with electrospray ionization. The measurements were done in a positive ion mode (interface capillary voltage 4.5 kV); mass range from m/z 50 to m/z 1600; external or internal calibration was done with Tuning Mix, Agilent. A syringe injection was used for the solutions in methanol (flow rate = 3 ml min^{-1}). Nitrogen was applied as a dry gas (flow rate =4 l min^{-1}); the interface temperature was set at 200 °C. The IR spectra were recorded using a BRUKER Vertex-70 FTIR spectrophotometer. UV-vis spectroscopy was performed using an Agilent 8453 instrument. The spectra were registered for 3×10^{-5} M solutions in MeCN in a 10 mm quartz cell. Differential thermal analysis (DTA) and thermogravimetry analysis (TGA) were performed on simultaneous thermal analyzer, DTG-60 (Shimadzu). All experiments were carried out under argon flow at a heating rate of 10 °C/min.

Cyclic voltammetry. Oxidation and reduction behaviors of **1–5** were analyzed by cyclic voltammetry using a digital potentiostat IPC-Pro-MF (Econix). Deaeration of solutions was performed by purging argon through them. To prevent the solution surface from contact with ambient air during the experiment, argon was constantly fed to the cell free space above the solution surface. The studied compounds dissolved in the supporting electrolyte (0.1 M Bu_4NPF_6/DMF) were electrochemically tested in a standard three-electrode glass cell. The working electrode was a glassy carbon disc electrode with a diameter of 1.7 mm. Before using, it was polished with abrasive paper and then GOI paste until the surface attained a mirror shine. The counter electrode was a Pt wire pre-annealed in a gas burner flame to remove oxides and other possible contaminations. The potentials of the studied processes were measured versus the Ag wire coated with AgCl (prepared by galvanostatic anodizing in 5% HCl solution) separated from the bulk electrolyte solution by an electrolytic bridge filled with the supporting electrolyte. The reference electrode was calibrated with respect to the ferrocene/ferrocenium couple (+0.33 V).

ESR spectroscopy. ESR measurements were performed on a Jeol JES-FA200 X-band spectrometer (JEOL Ltd., Tokyo, Japan) using a Jeol X-Band microwave setup (Tokyo, Japan) at room temperature. Solutions of anion radicals in DMF were generated electrochemically in a glovebox. The solution was placed using a syringe with a needle into a glass capillary sealed at one end with an inner diameter of 1 mm and a liquid column height of 25 mm. The capillary was hermetically sealed from the environment with parafilm and placed in a standard NMR ampoule,

which was also carefully wrapped in parafilm. The ampoule was removed from the glovebox, after which the spectrum was recorded no later than 1 hour after preparation. (The spectra remained unchanged during this time interval.) The spectra were recorded in a single slow (~30 min) scan with a modulation of 0.16 mT at a frequency of 100 kHz and a power of 4 mW. The isotropic g-factor values were measured experimentally using Mn(II)-doped MgO as a standard placed in the resonator simultaneously with the studied solution. The spectra were simulated using the EasySpin package for Matlab.

X-ray Crystallography. X-ray diffraction data were collected at 100K on a Bruker Quest D8 diffractometer equipped with a Photon-III area-detector (graphite monochromator, shutterless φ- and ω-scan technique), using Mo K_α-radiation. The intensity data were integrated by the SAINT program[1] and were semi-empirically corrected for absorption and decay from equivalent reflections by multi-scan methods using SADABS.[2] The structure was solved by dual methods using SHELXT-2014/5[3] and refined by the full-matrix least-squares minimization method on F^2 using SHELXL-2018/3.[4] All non-hydrogen atoms were refined with individual anisotropic displacement parameters. Locations of atoms H5 and H6 (at nitrogen atoms) were found from the electron density-difference map; these hydrogen atoms were refined with individual isotropic displacement parameters. All other hydrogen atoms were placed in ideal calculated positions and refined as riding atoms with relative isotropic displacement parameters. The Mercury program[5] was used for molecular graphics. The crystallographic data and structure refinement details for **2** are given in Table S1.

CCDC 2491385 contain the supplementary crystallographic data for this paper. These data can be obtained free of charge via https://www.ccdc.cam.ac.uk/structures/, or by emailing data_request@ccdc.cam.ac.uk, or by contacting The Cambridge Crystallographic Data Centre, 12 Union Road, Cambridge CB2 1EZ, UK; fax: +44 1223 336033.

Table S1. The crystallographic data and structure refinement details for **2**.

Empirical formula	$C_{30}H_{28}N_6S_2Sn$	
Formula weight	655.39	
Temperature	100(2) K	
Wavelength	0.71073 Å	
Crystal system	Triclinic	
Space group	$P\bar{1}$	
Unit cell dimensions	a = 8.5688(9) Å b = 11.3820(12) Å c = 15.1663(16) Å	α = 108.959(3)° β = 93.759(3)° γ = 100.386(3)°
Volume	1363.7(3) $Å^3$	
Z	2	
Density (calculated)	1.596 $g \cdot cm^{-3}$	
Absorption coefficient	1.123 mm^{-1}	
F(000)	664	
Crystal size	0.249 × 0.122 × 0.078 mm	
Theta range for data collection	2.438 to 30.508°.	
Index ranges	$-12 \le h \le 12$, $-16 \le k \le 16$, $-21 \le l \le 21$	
Reflections collected	38556	
Independent reflections	8277 [R(int) = 0.1339]	
Observed reflections with I>2σ(I)	5418	
Completeness to θ_{full} / θ_{max}	0.989 / 0.992	
Max. and min. transmission	0.4942 and 0.4136	
Data / restraints / parameters	8277 / 0 / 363	
Goodness-of-fit on F^2	1.023	
R indices [I>2σ(I)]	R_1 = 0.0649 / ωR_2 = 0.1262	
R indices (all data)	R_1 = 0.1201 / ωR_2 = 0.1498	
Extinction coefficient	0.0040(7)	
Largest diff. peak / hole	1.300 / -1.628 $e \cdot Å^{-3}$	

S2. Synthesis of ligands

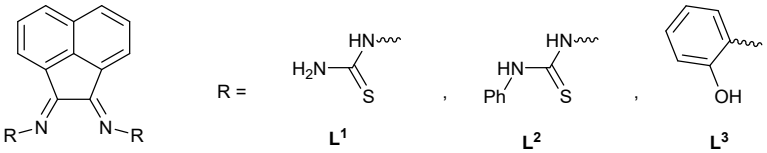

General procedure. The thiosemicarbazone derivatives were prepared by refluxing acenaphtenequinone and thiosemicarbazide hydrochloride or phenylthiosemicarbazide in ratio 1:2 in methanol with HCl catalysis. The structure of synthesized compounds was confirmed by NMR, IR spectroscopy and MS-spectrometry.

L^1. Yield 76%. ^{1}H NMR (DMSO-d_6, δ): 12.44 (s, 1H), 11.21 (s, 1H), 8.80 (br s, 2H), 8.57 (s, 1H), 8.21–7.99 (m, 5H), 7.90–7.33 (m, 2H).

^{13}C NMR (DMSO-d_6, δ): 180.85, 178.91, 137.97, 136.20, 132.80, 129.91, 129.00 (CH), 128.58 (CH), 128.17 (CH), 127.81, 126.75 (CH), 124.73 (CH), 118.61 (CH).

IR: 3444, 3411, 3252, 3158, 1596, 1512, 1479, 1453, 1425, 1360, 1264, 1184, 1166, 1139, 1111, 1083, 1057, 9+56, 929, 892, 837, 822, 779, 632, 612, 541, 502, 423.

MS: 328 (4) $[M]^+$, 311 (3) $[M\text{-}NH_3]^+$, 253 (100) $[M\text{-}NH_2CSNH]^+$, 237 (2), 213 (8), 180 (6), 164 (16), 152 (24), 139 (8), 60 (100).

L^2. Yield 81%. ^{1}H NMR (DMSO-d_6, δ): 12.96 (s, 1H, NH), 11.55 (s, 1H, NH), 10.74 and 10.68 (s and s, 2H, NH), 8.33–8.28 (t, 2H, J = 7.5 Hz), 8.19–8.16 (d, 1H, J = 8.3 Hz), 8.08–8.06 (d, 1H, J = 8.2 Hz), 7.88–7.78 (m, 4H), 7.70–7.67 (d. 2H, J = 7.7 Hz), 7.47–7.39 (m, 4H), 7.33–7.21 (m, 2H).

^{13}C NMR (DMSO-d_6, δ): 178.41, 176.56, 138.89, 138.81, 138.38, 136.30, 132.69, 129.97, 129.10 (CH), 128.59 (CH), 128.32 (CH), 128.29 (CH), 128.20 (CH), 127.75, 126.95 (CH), 125.77 (CH), 125.65 (CH), 125.37 (CH), 124.71 (CH), 124.22 (CH), 119.20 (CH).

IR: 3446, 3277, 1597, 1551, 1532, 1493, 1475, 1442, 1393, 1375, 1354, 1287, 1179, 1152, 1139, 1098, 887, 820, 768, 749, 687, 649, 588, 492.

MS: 412 (0.5) $[M\text{-}68]^+$, 353(2) $[M\text{-}C_{10}H_7]^+$, 329 (1) $[M\text{-}C_{12}H_7]^+$, 295 (4) $[C_{14}H_{11}N_6S]^+$, 268 (2) $[C_{13}H_{10}N_5S]^+$, 237 (8) $[C_{13}H_7N_3S]^+$, 209 (10) $[C_{12}H_8N_2]^+$, 178 (8) $[C_{12}H_6N_2]^+$, 164 (14), 151 (8), 135 (13), 118 (7), 93 (90), 77 (54), 66 (76), 51 (80), 39 (100).

S3. Spectral data for ligands

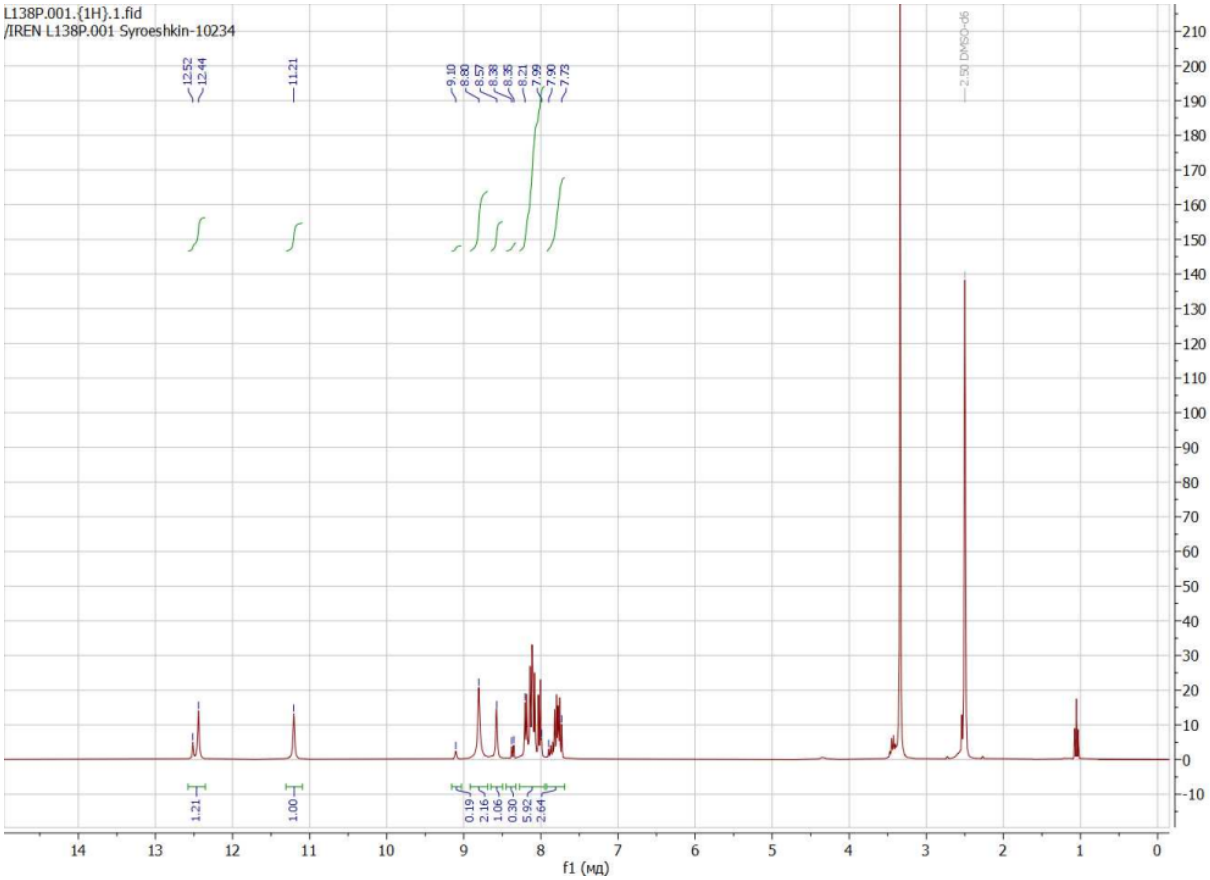

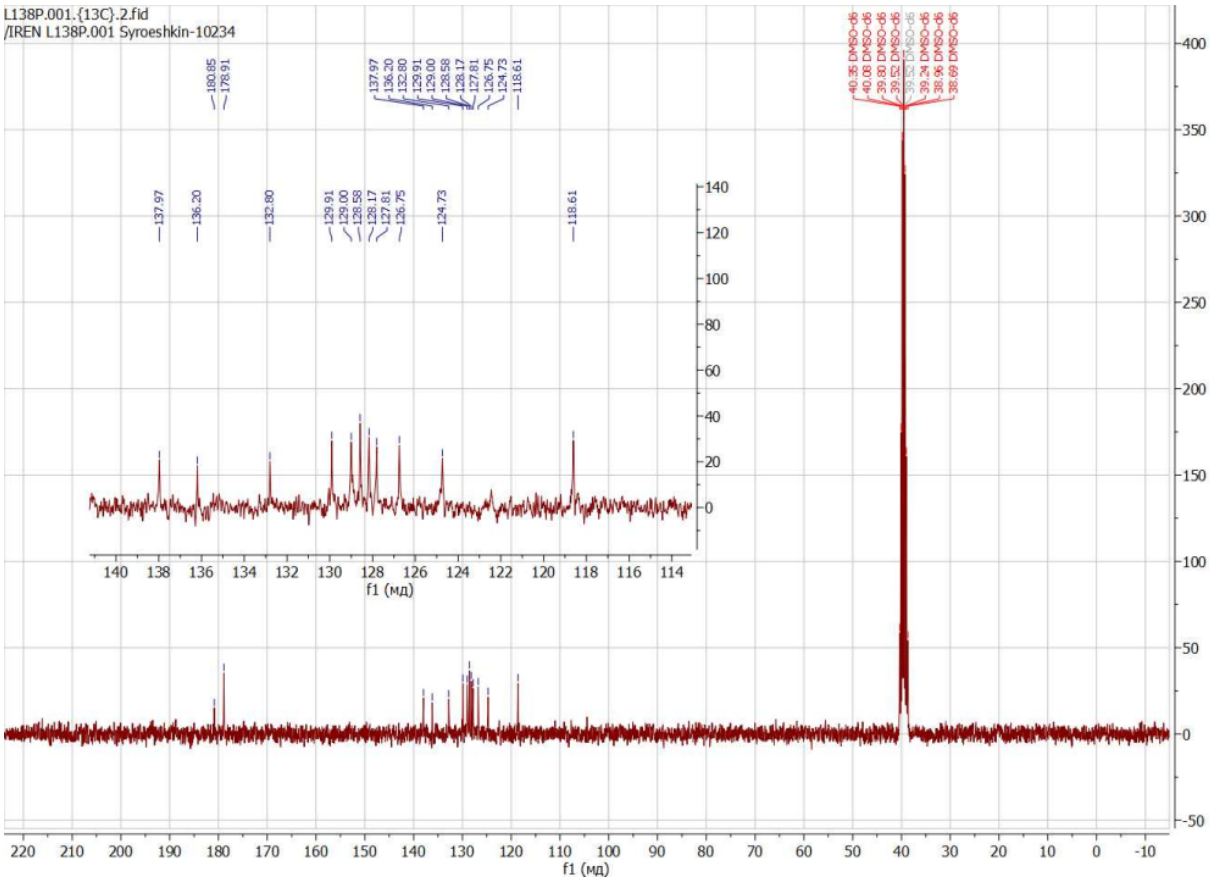

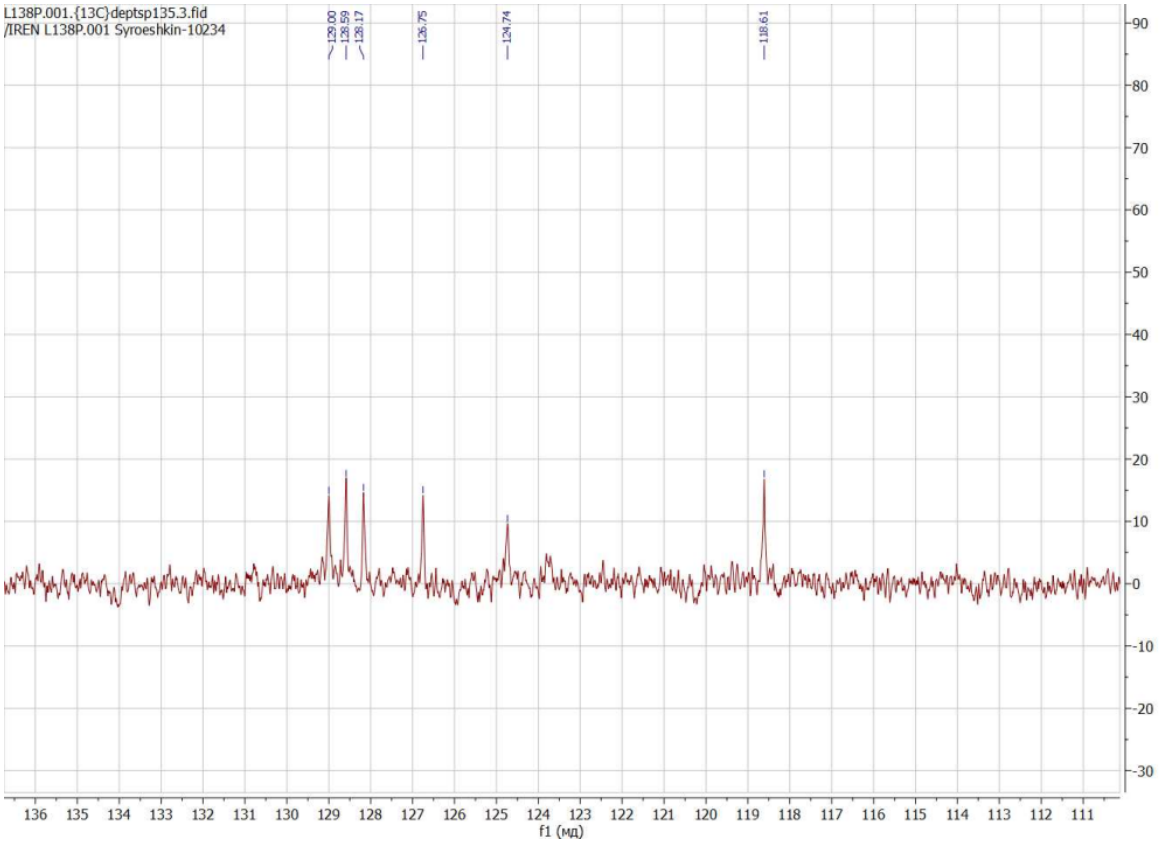
L138P.001.{13C}deptsp135.3.fid
/IREN L138P.001 Syroeshkin-10234
129.00
128.59
128.17
126.75
124.74
118.61
f1 (мд)

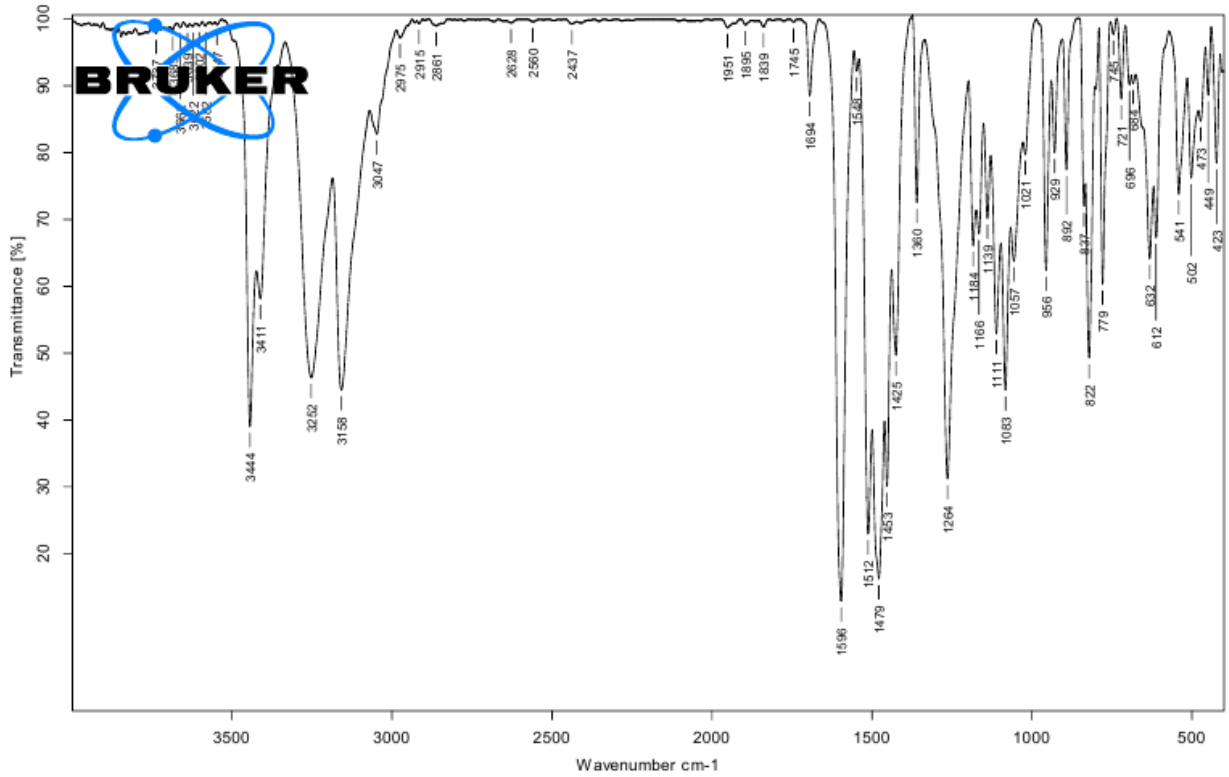
BRUKER
Transmittance [%]
Wavenumber cm-1
3444
3411
3252
3158
3047
2975
2915
2861
2628
2560
2437
1951
1895
1839
1745
1694
1596
1548
1512
1479
1453
1425
1360
1264
1184
1166
1139
1111
1083
1057
1021
956
929
892
837
822
779
745
721
696
684
632
612
541
502
473
449
423

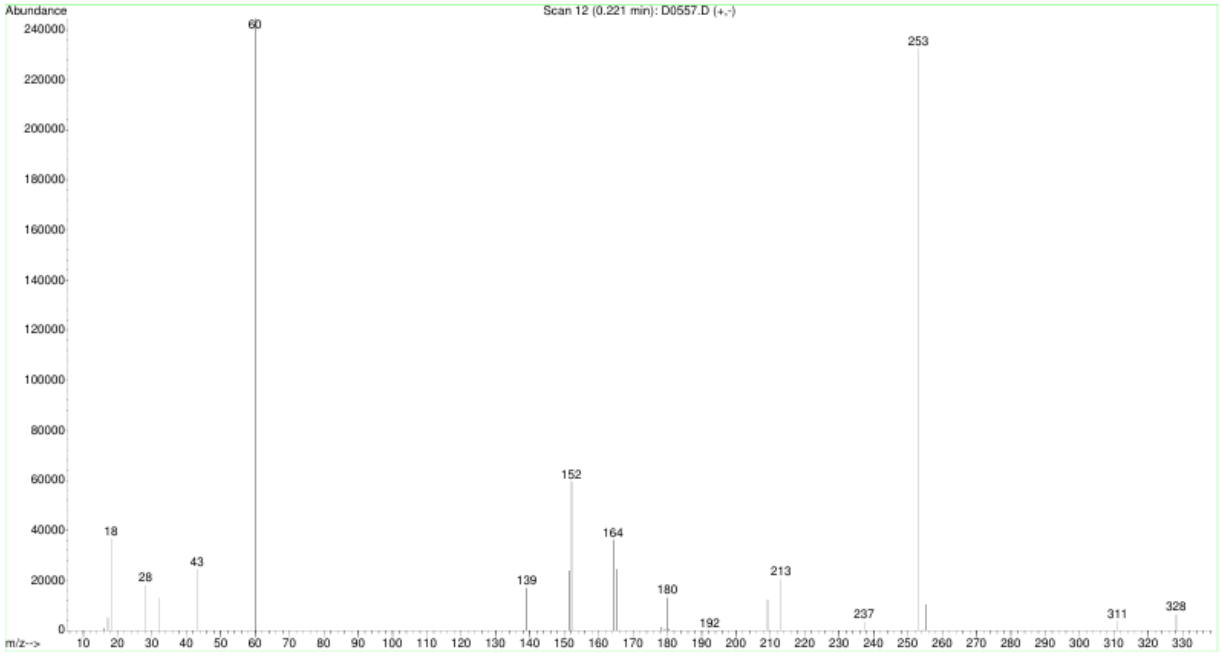

Figure S1. NMR, IR, and mass spectra for $\mathbf{L^1}$.

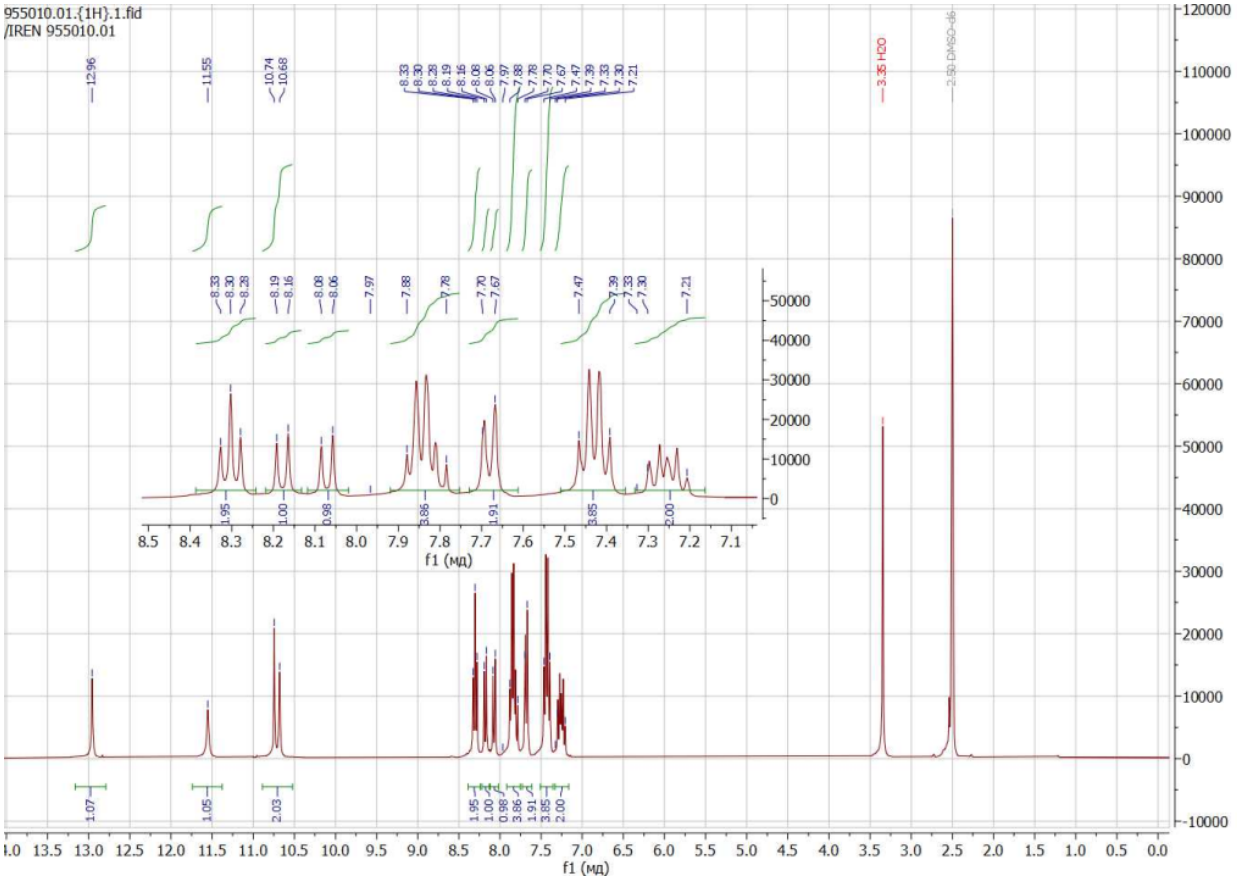
955010.01.{1H}.1.fid
/IREN 955010.01
f1 (мд)

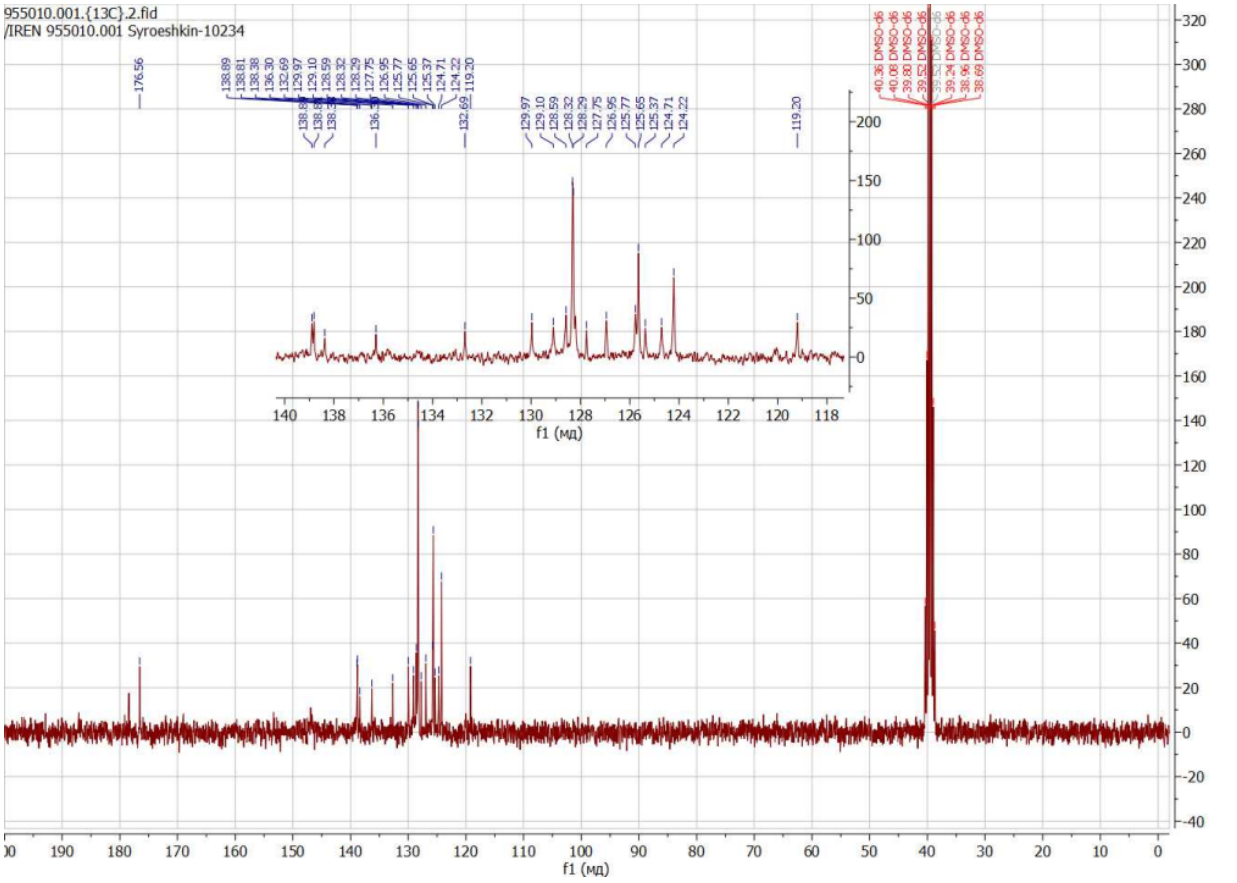
955010.001.{13C}.2.fid
/IREN 955010.001 Syroeshkin-10234
f1 (мд)

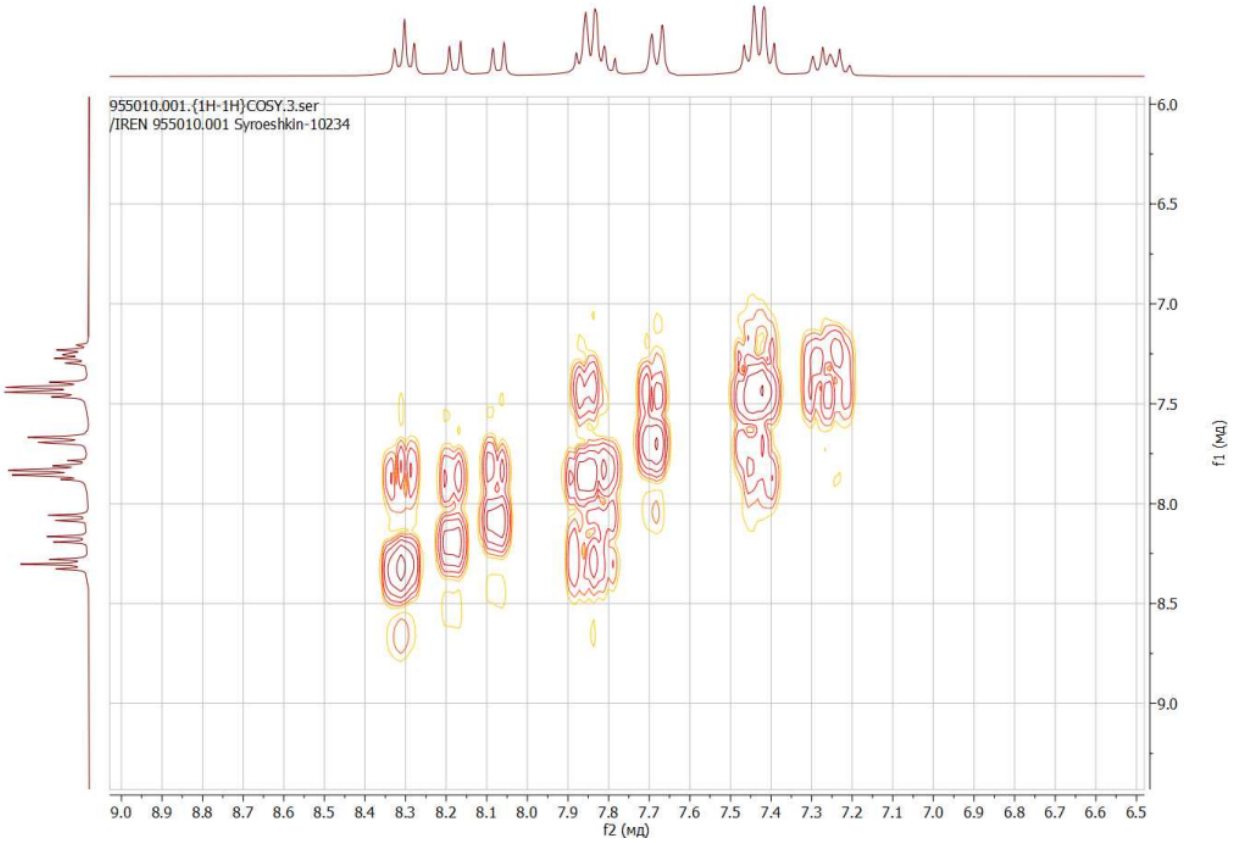
955010.001.{1H-1H}COSY.3.ser
/IREN 955010.001 Syroeshkin-10234
f2 (мд)
f1 (мд)

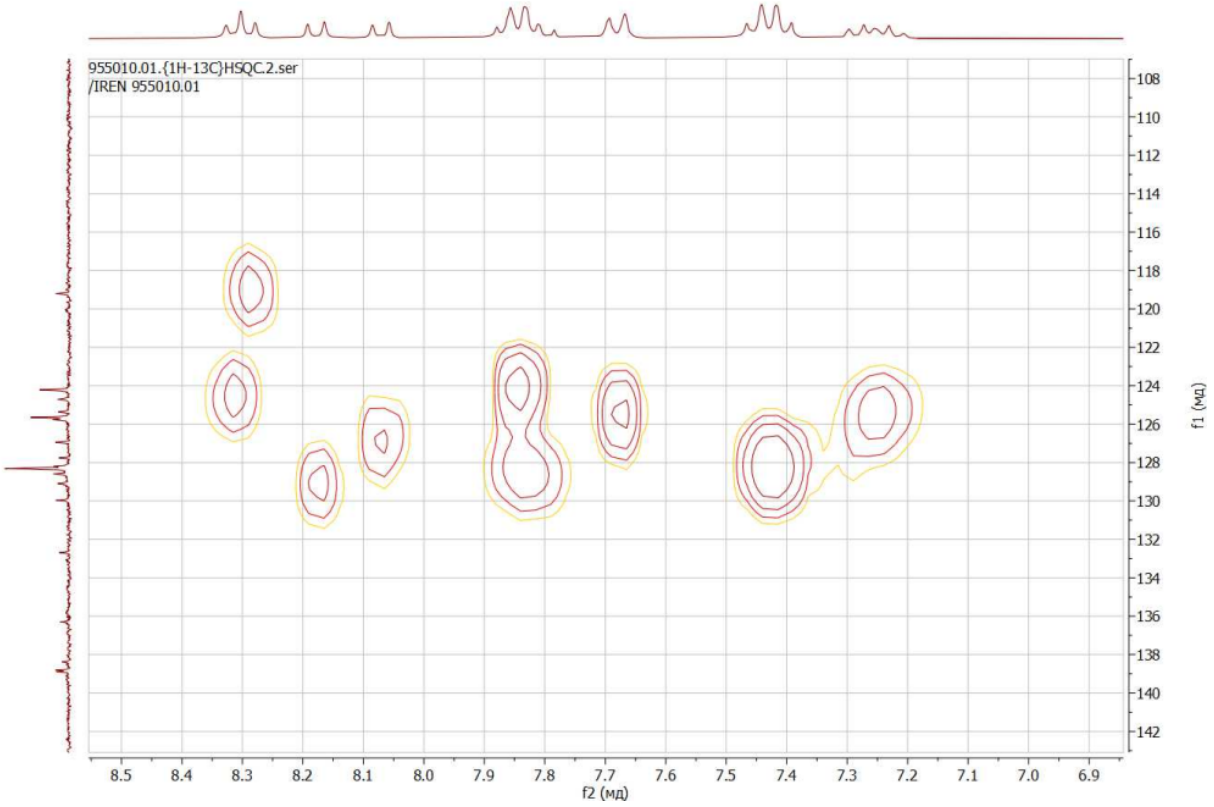
955010.01.{1H-13C}HSQC.2.ser
/IREN 955010.01
f2 (мд)
f1 (мд)

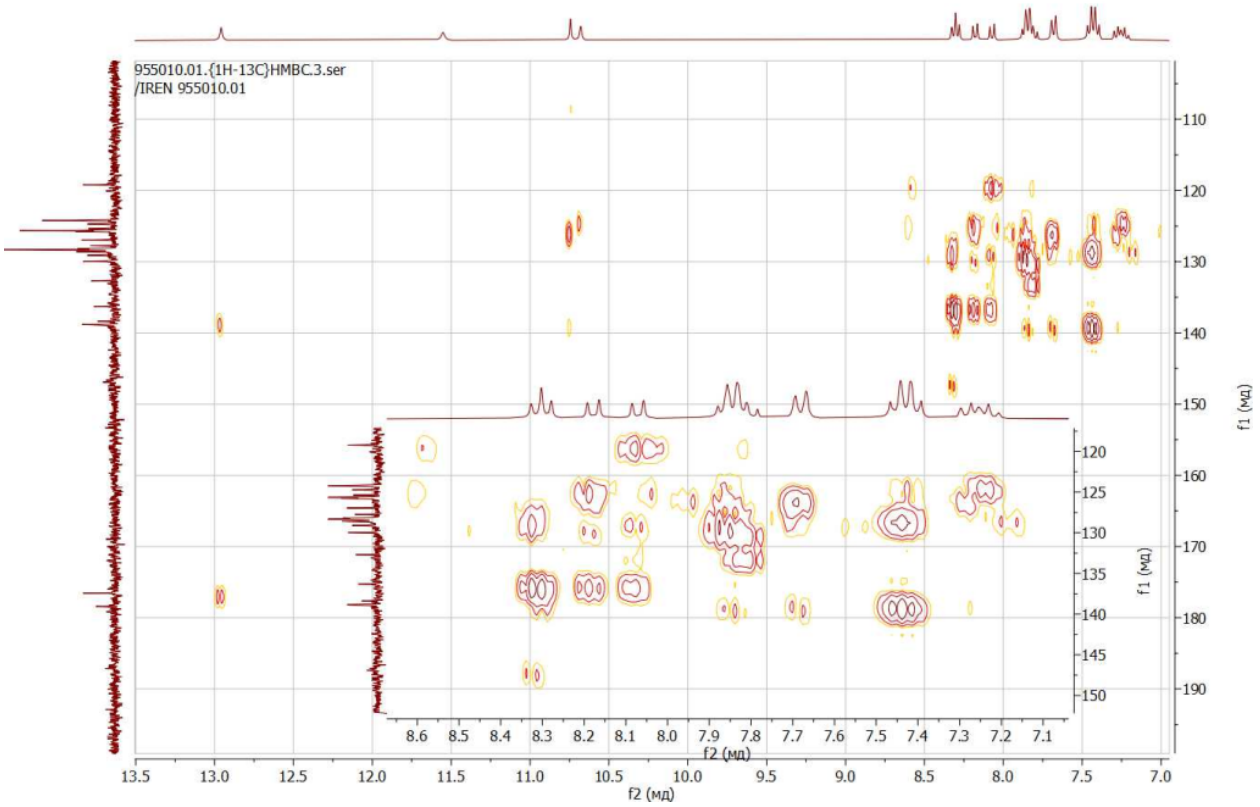
955010.01.{1H-13C}HMBC.3.ser
/IREN 955010.01
f2 (мд)
f1 (мд)

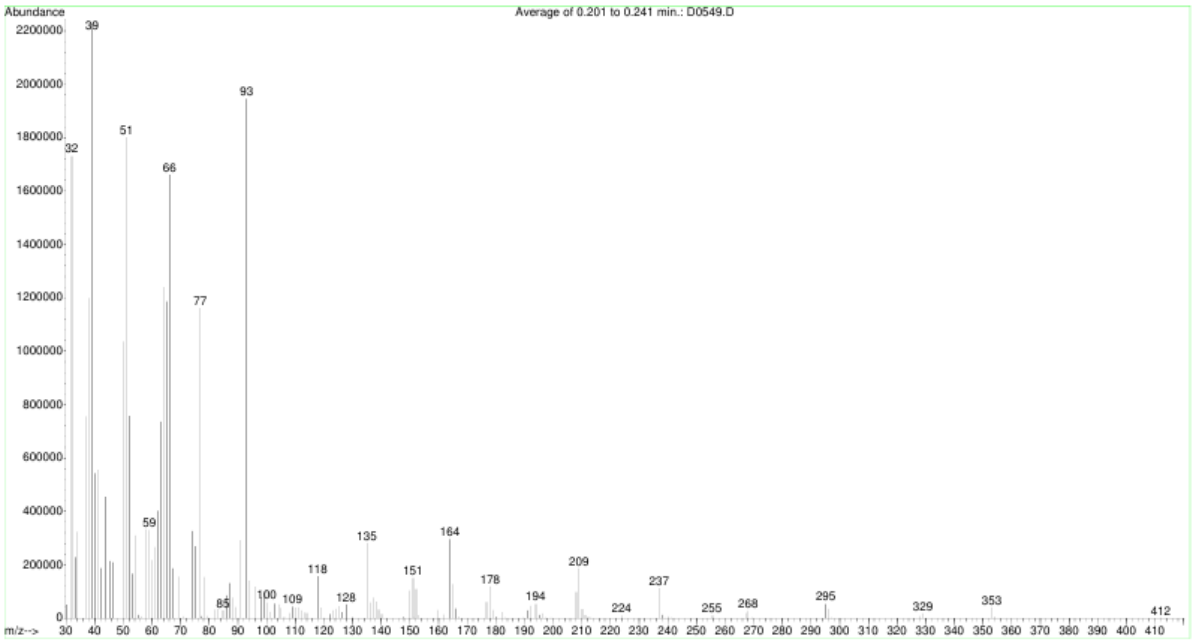
Abundance
Average of 0.201 to 0.241 min.: D0549.D
m/z-->

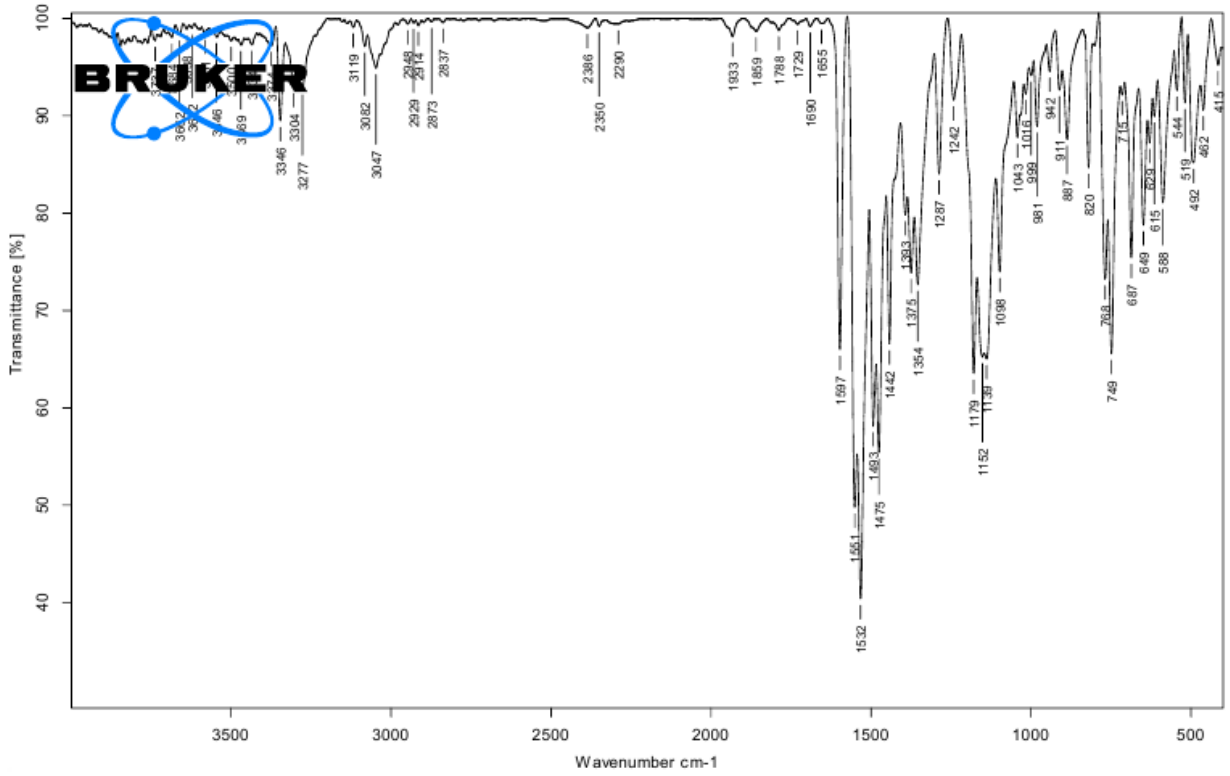

Figure S2. NMR, IR, and mass spectra for **L²**.

S4. Spectroscopic data for complexes

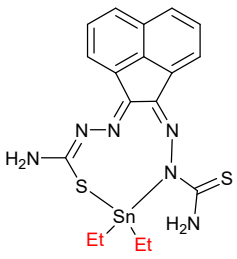

1

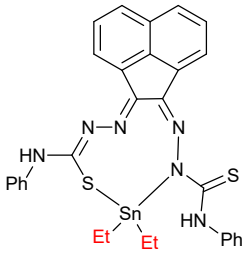

2

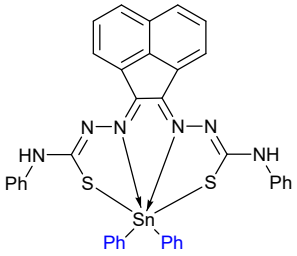

3

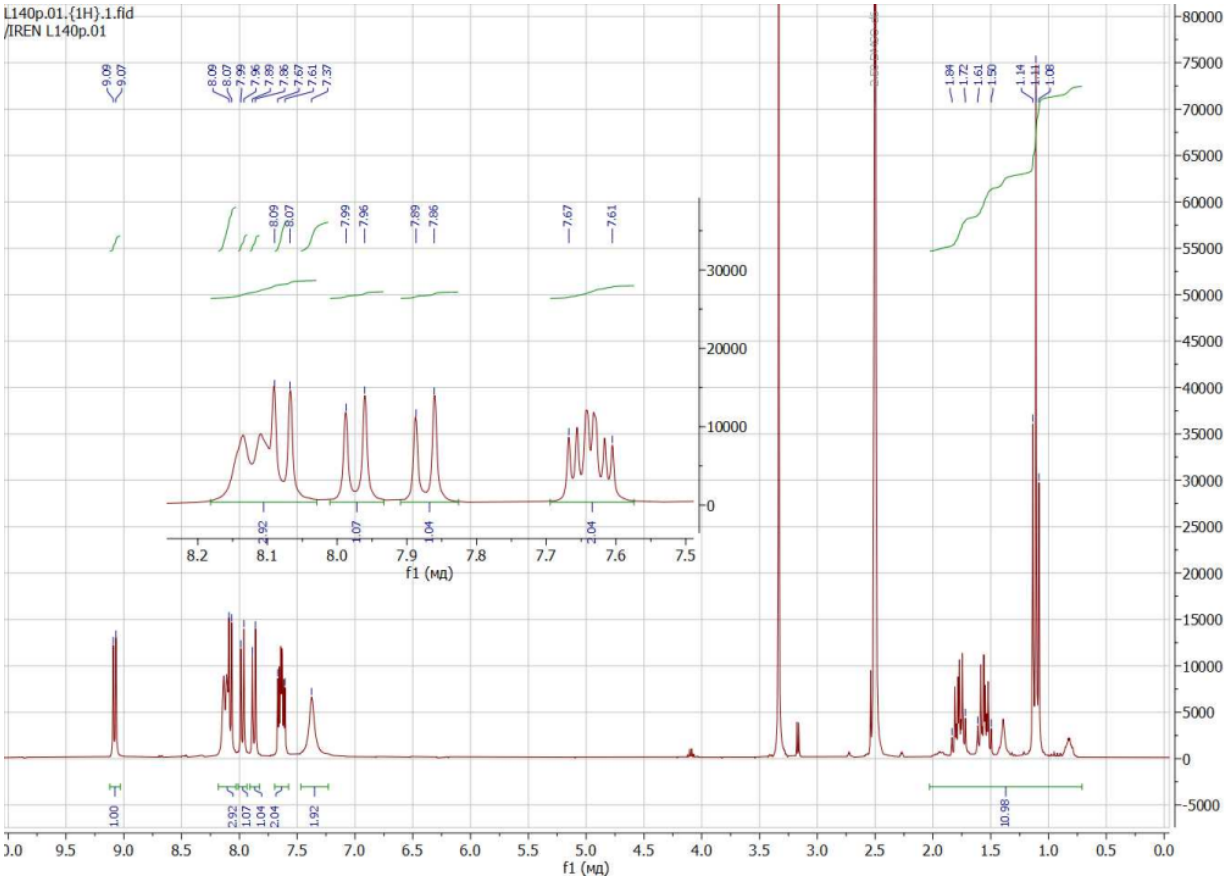

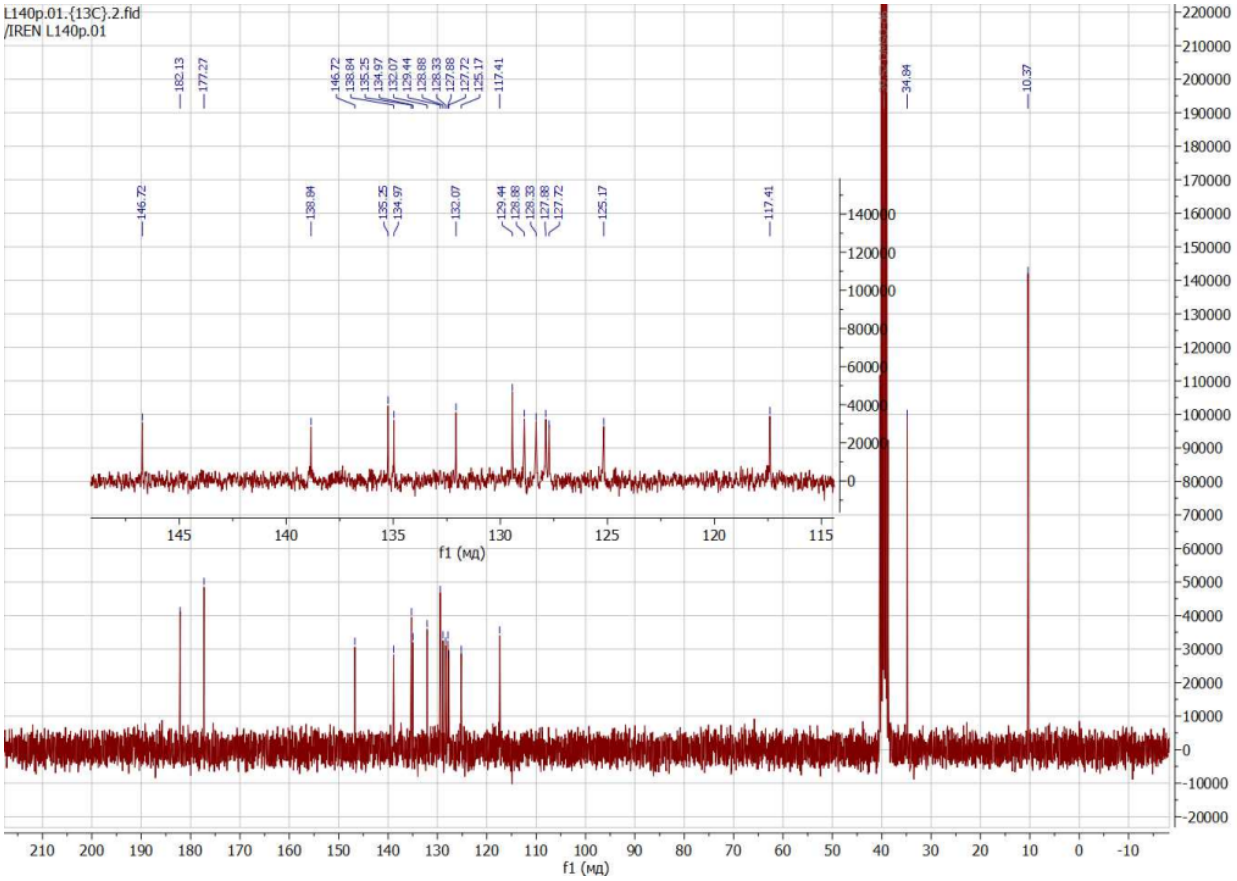
L140p.01.{13C}.2.fid
/IREN L140p.01
182.13
177.27
146.72
138.84
135.25
134.97
132.07
129.44
128.88
128.33
127.88
127.72
125.17
117.41
34.84
10.37
f1 (мд)

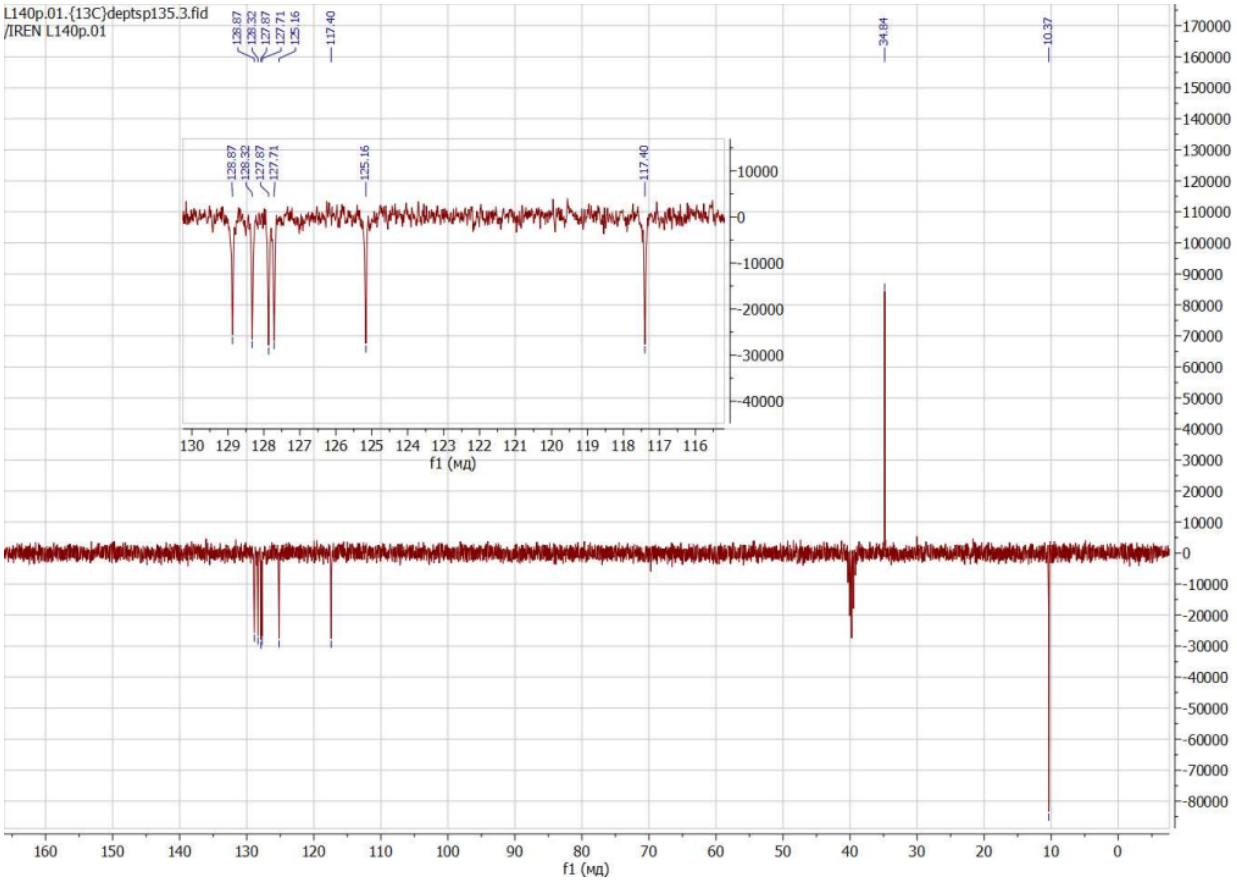
L140p.01.{13C}deptsp135.3.fid
/IREN L140p.01
128.87
128.32
127.87
127.71
125.16
117.40
34.84
10.37
f1 (мд)

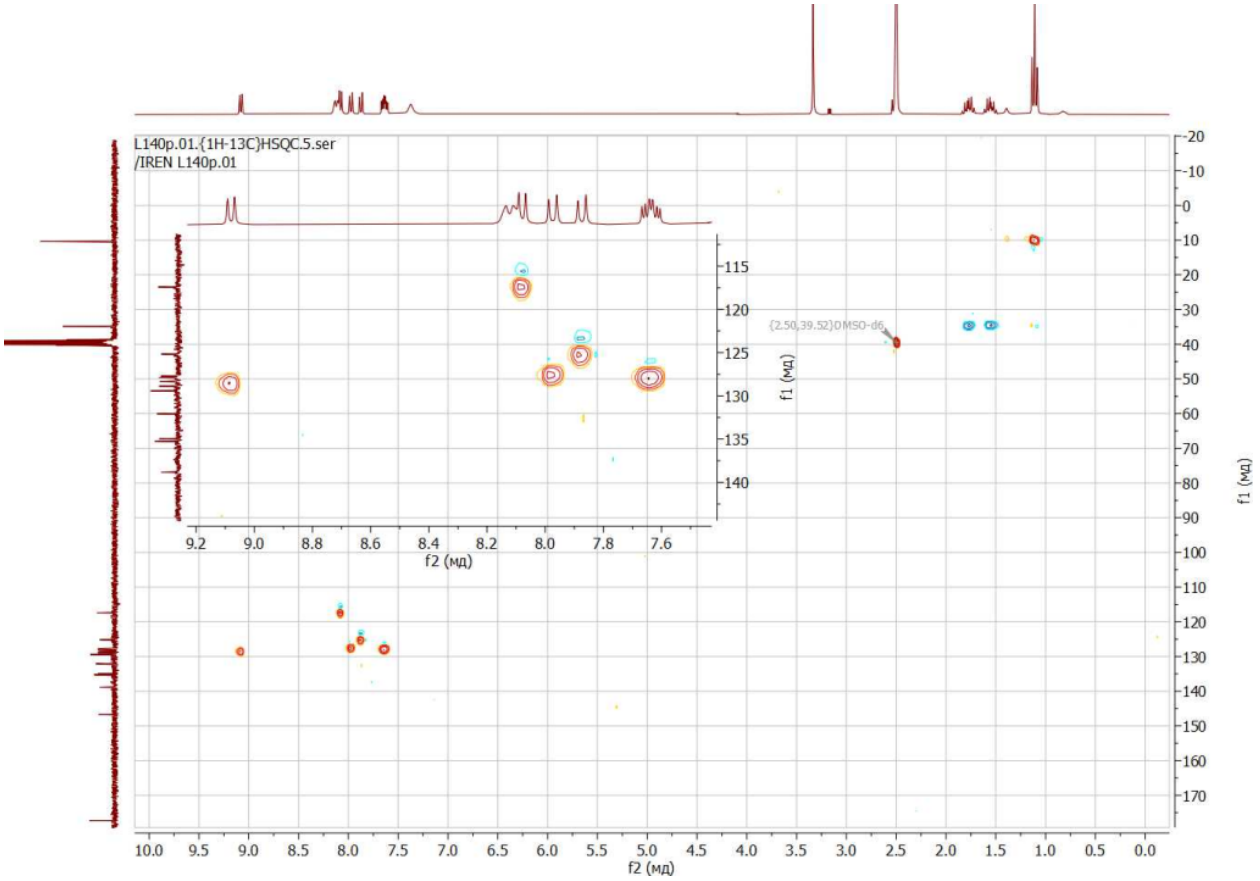
L140p.01.{1H-13C}HSQC.5.ser
/IREN L140p.01
{2.50,39.52}DMSO-d6
f1 (мд)
f2 (мд)

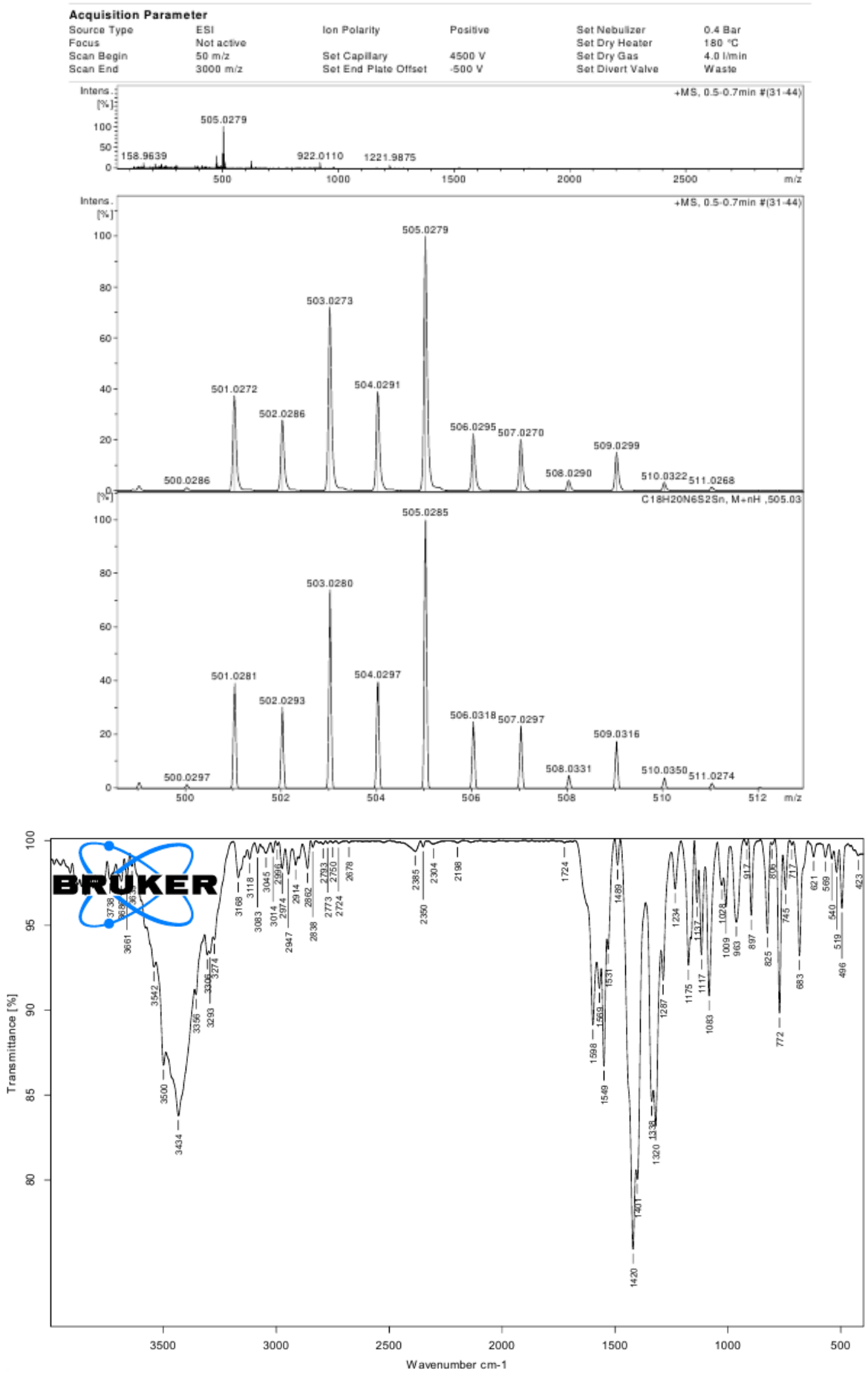

Figure S3. NMR, IR, and mass spectra for complex **1**.

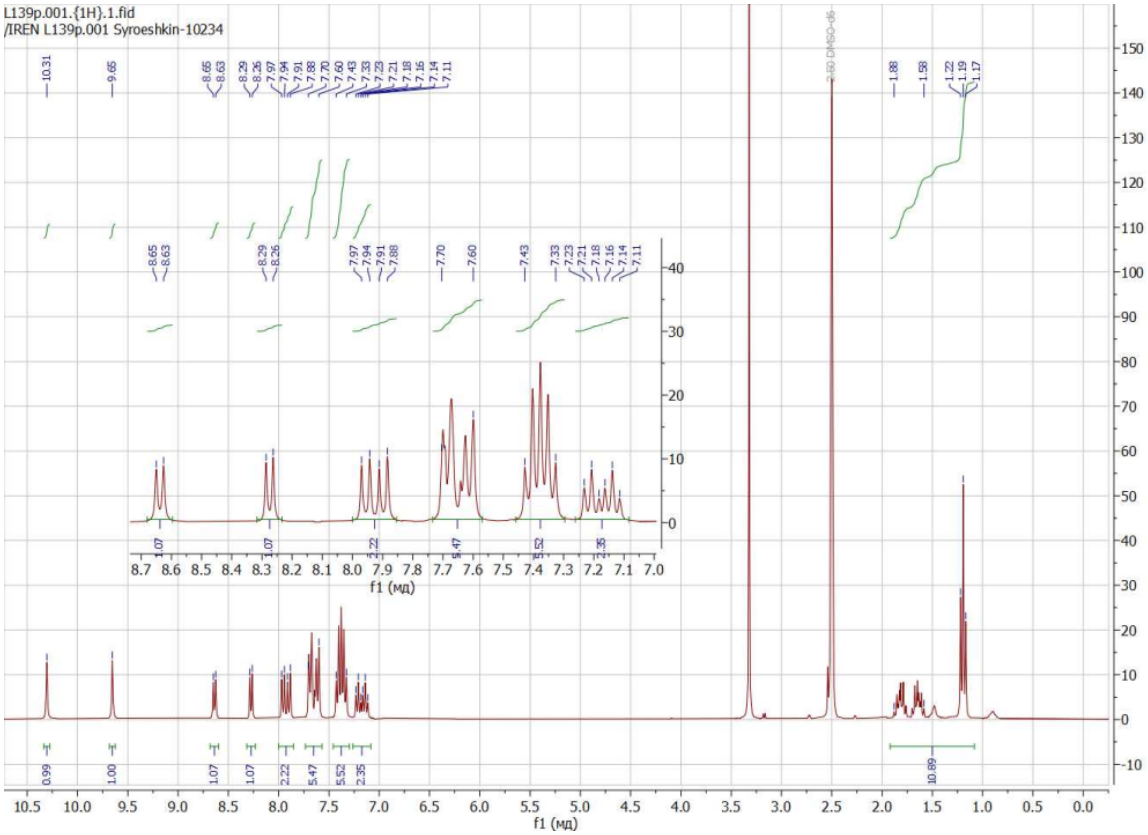
L139p.001.{1H}.1.fid
/IREN L139p.001 Syroeshkin-10234
f1 (мд)

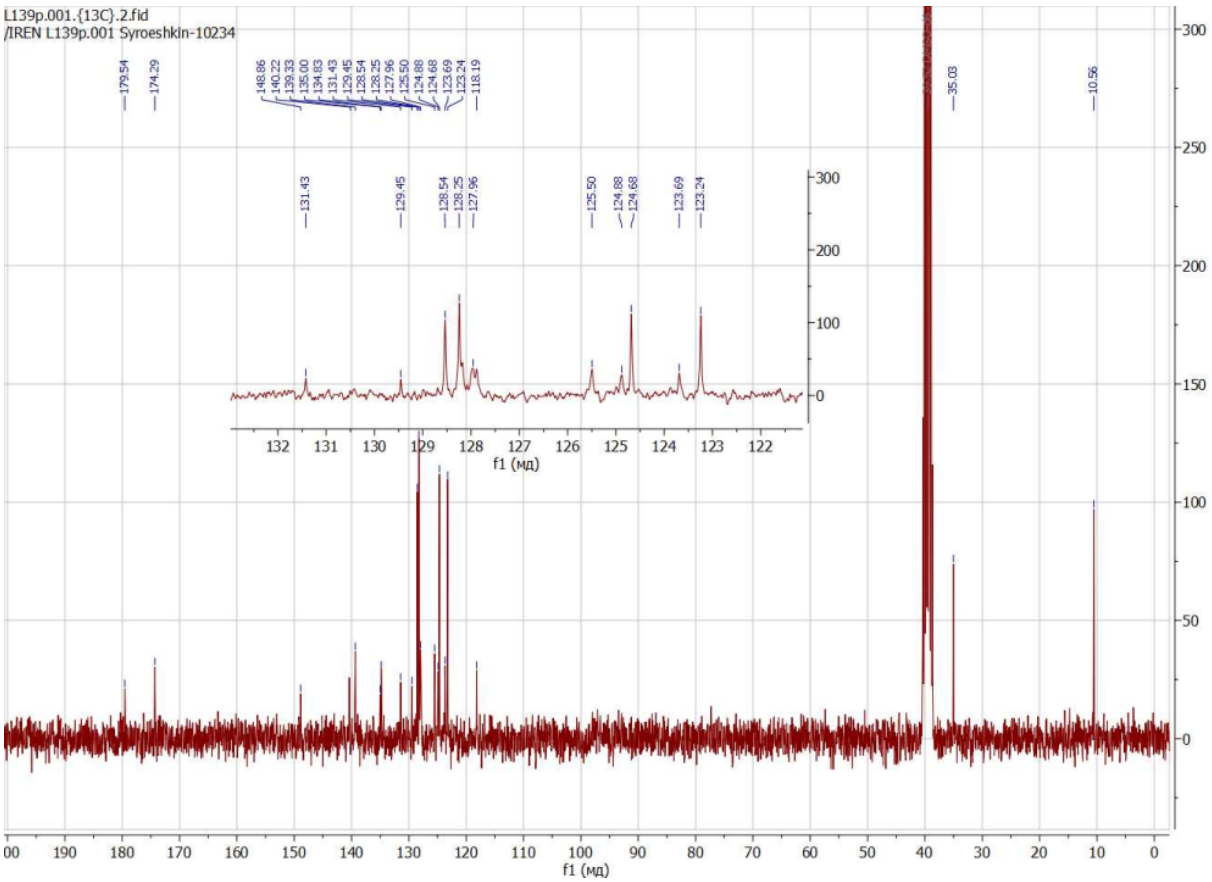
L139p.001.{13C}.2.fid
/IREN L139p.001 Syroeshkin-10234
f1 (мд)

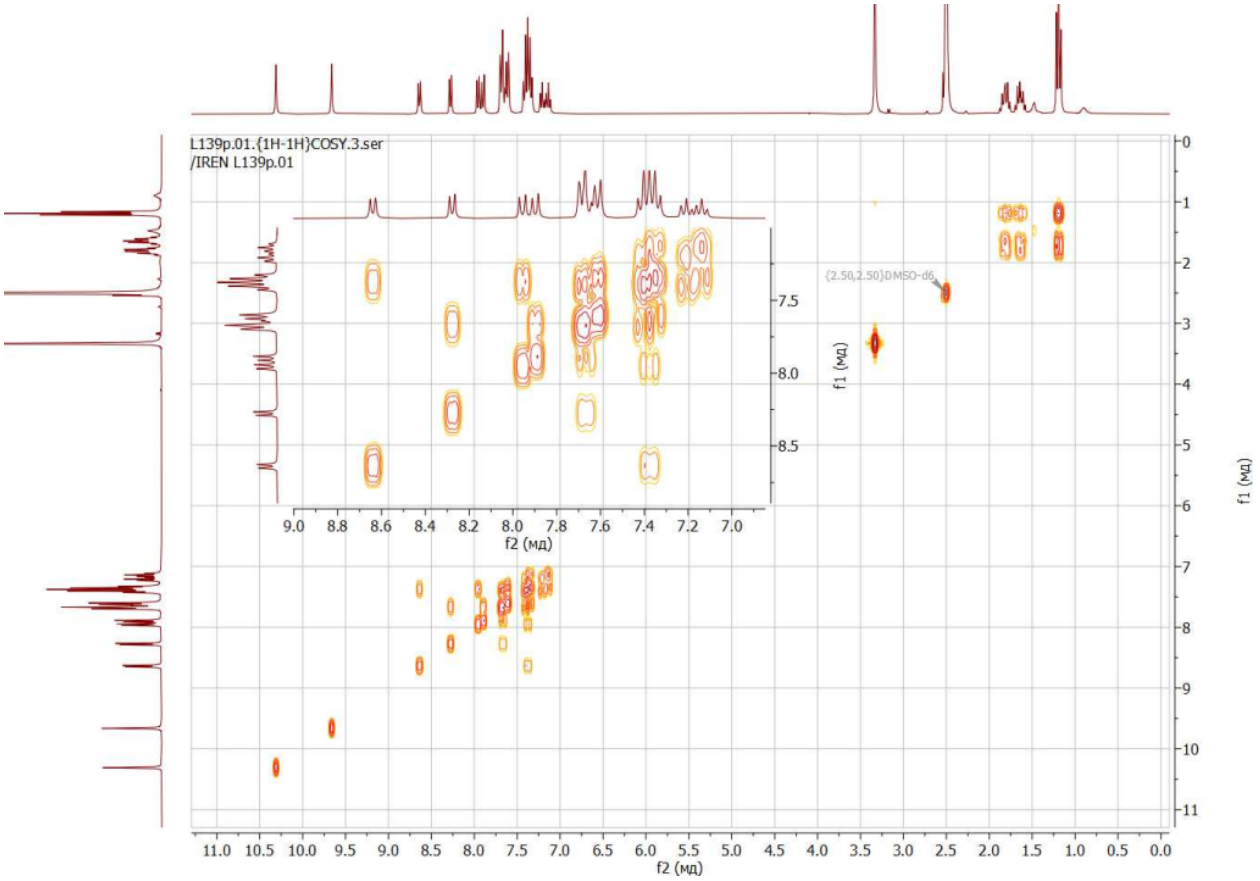
L139p.01.{1H-1H}COSY.3.ser
/IREN L139p.01
{2.50,2.50}DMSO-d6
f1 (мд)
f2 (мд)

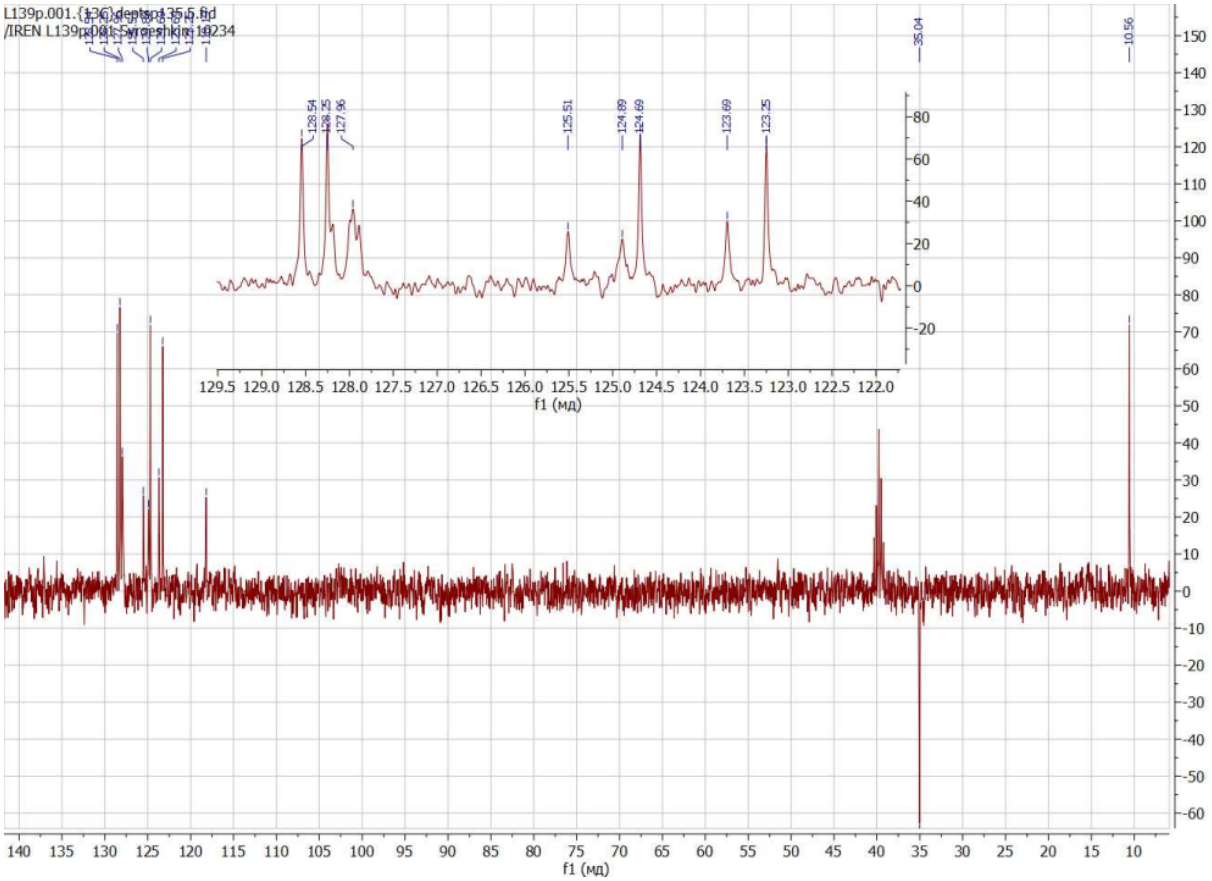
L139p.001.{13C}dept
/IREN L139p.001
128.54
128.25
127.96
125.51
124.89
124.69
123.69
123.25
35.04
10.56
f1 (мд)

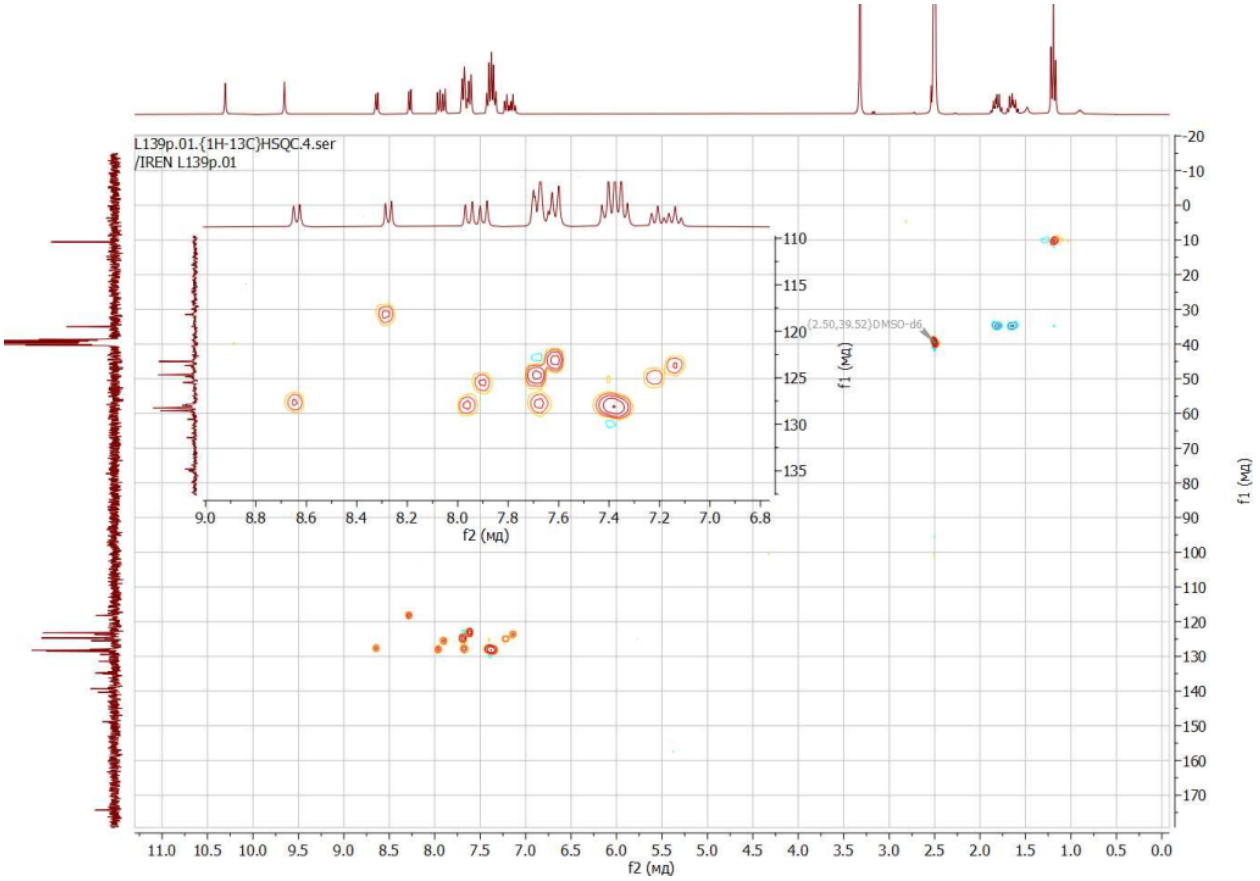
L139p.01.{1H-13C}HSQC.4.ser
/IREN L139p.01
f2 (мд)
f1 (мд)
(2.50,39.52)DMSO-d6

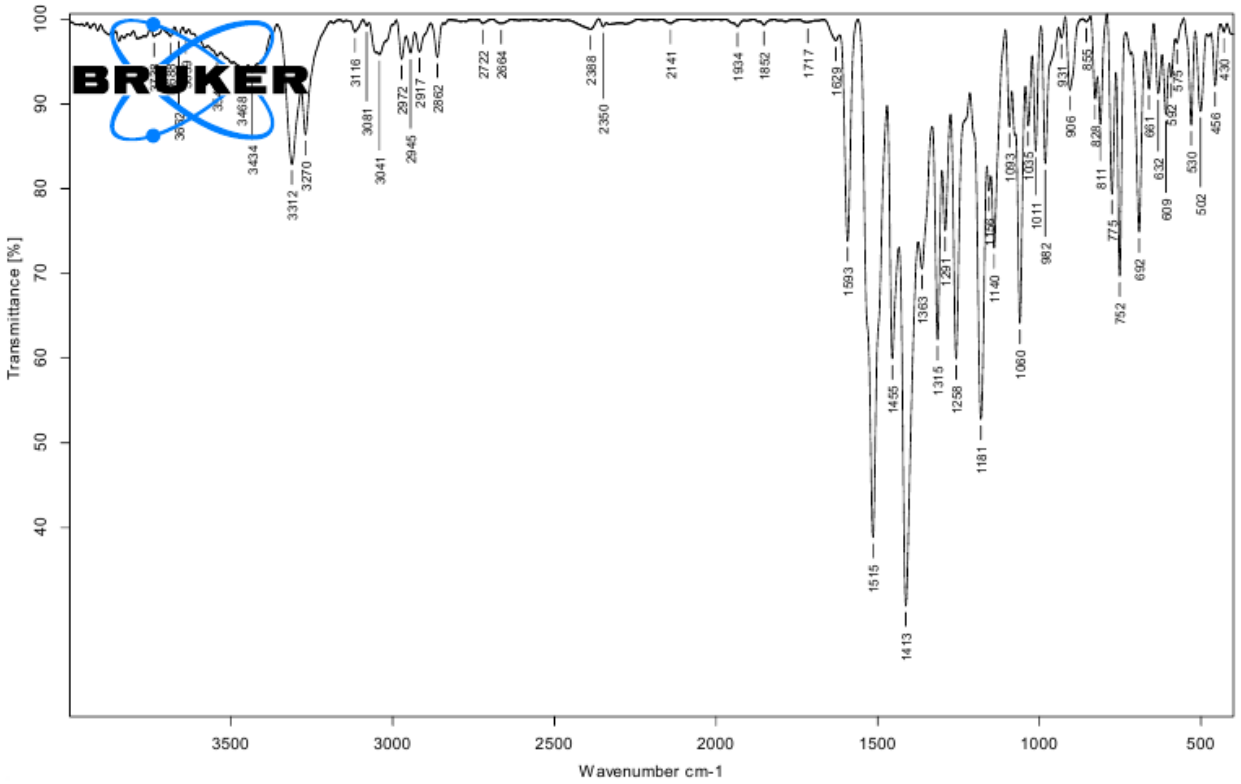
BRUKER
Transmittance [%]
Wavenumber cm-1

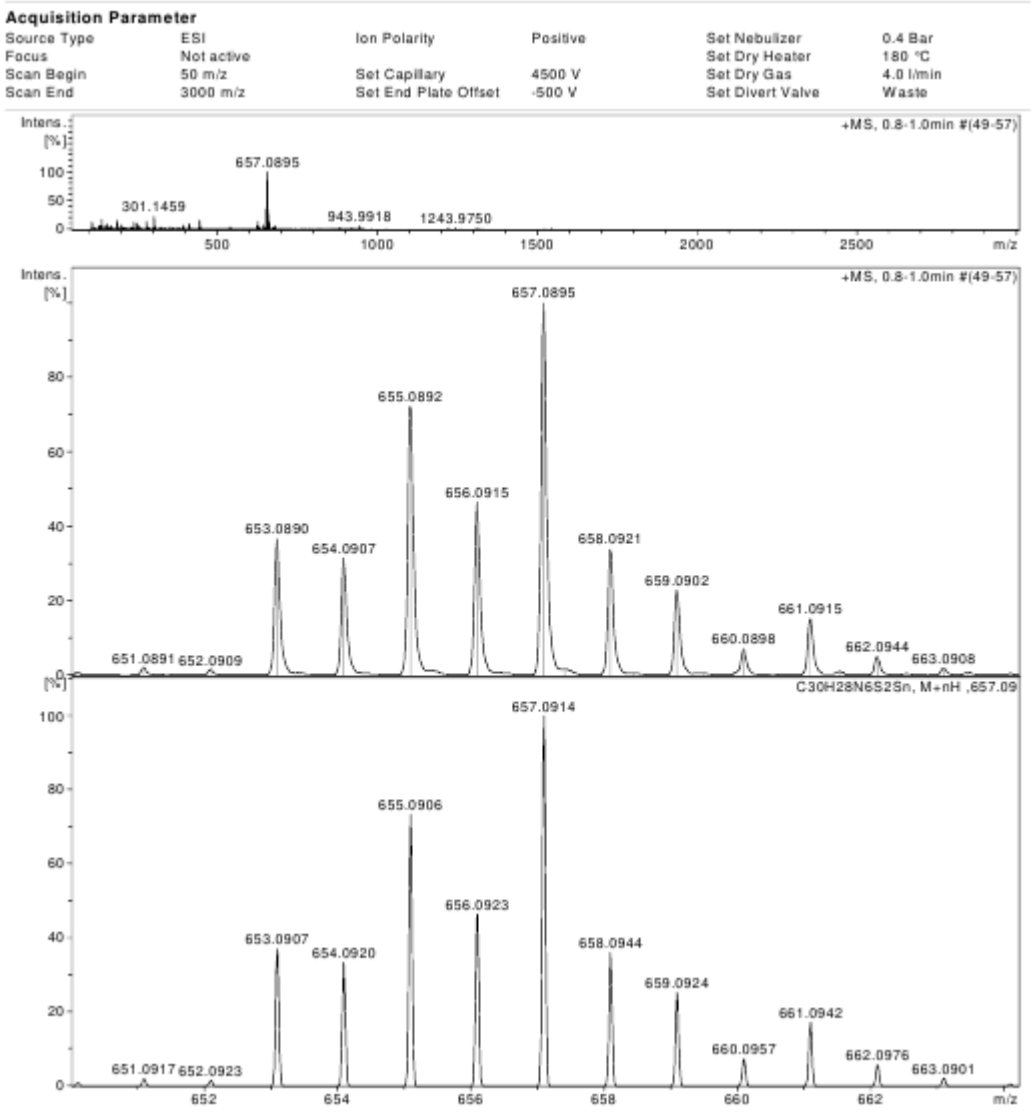

Figure S4. NMR, IR, and mass spectra for complex **2**.

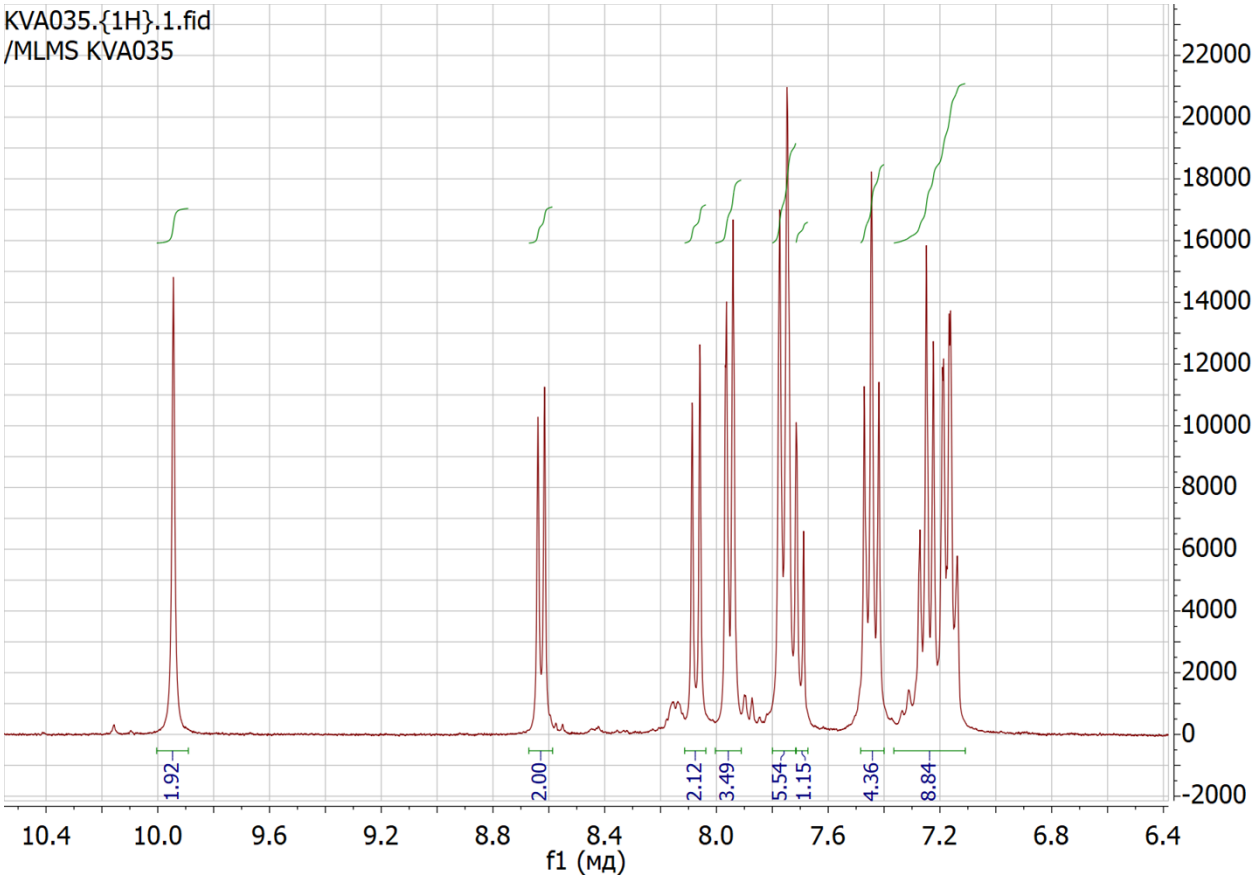
KVA035.{1H}.1.fid
/MLMS KVA035
22000
20000
18000
16000
14000
12000
10000
8000
6000
4000
2000
0
-2000
1.92
2.00
2.12
3.49
5.54
1.15
4.36
8.84
10.4
10.0
9.6
9.2
8.8
8.4
8.0
7.6
7.2
6.8
6.4
f1 (мд)

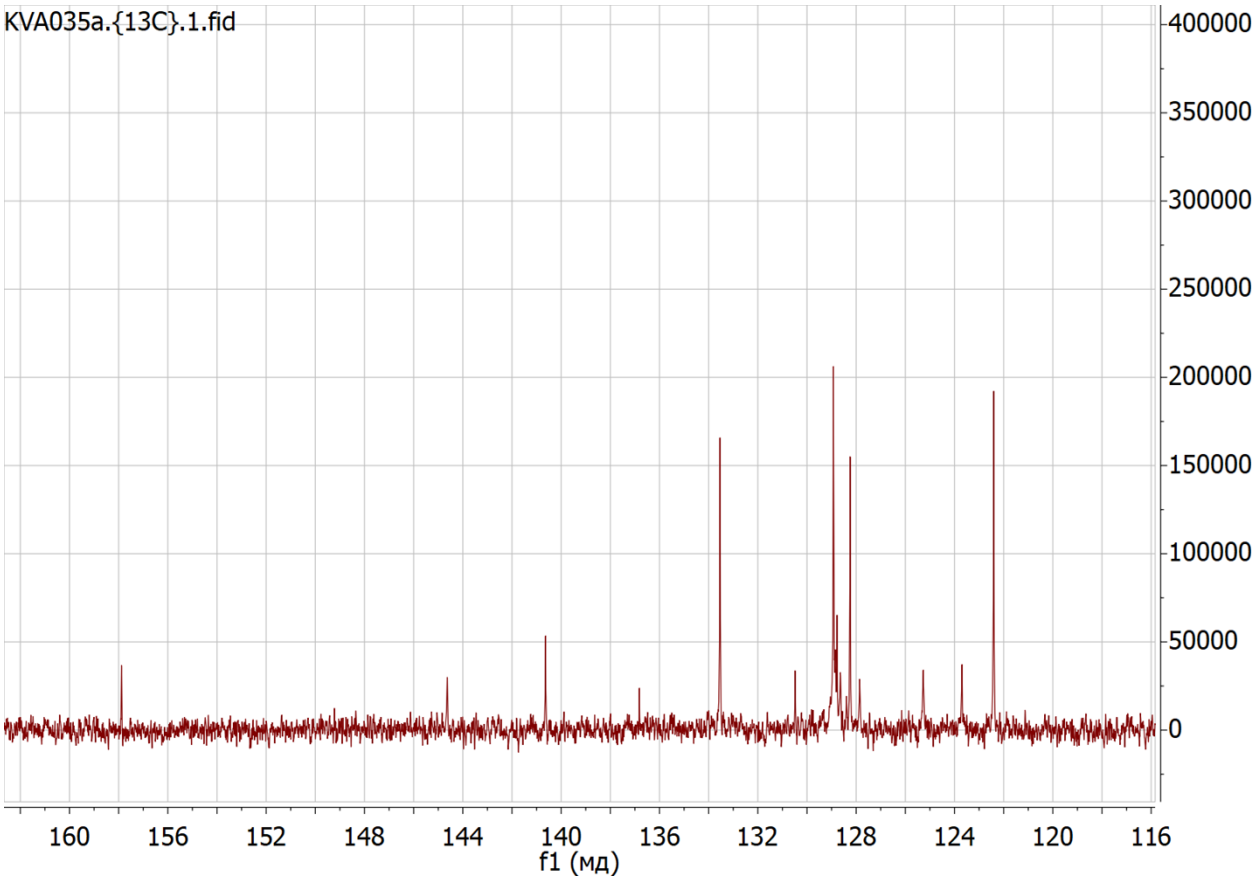
KVA035a.{13C}.1.fid
400000
350000
300000
250000
200000
150000
100000
50000
0
160
156
152
148
144
140
136
132
128
124
120
116
f1 (мд)

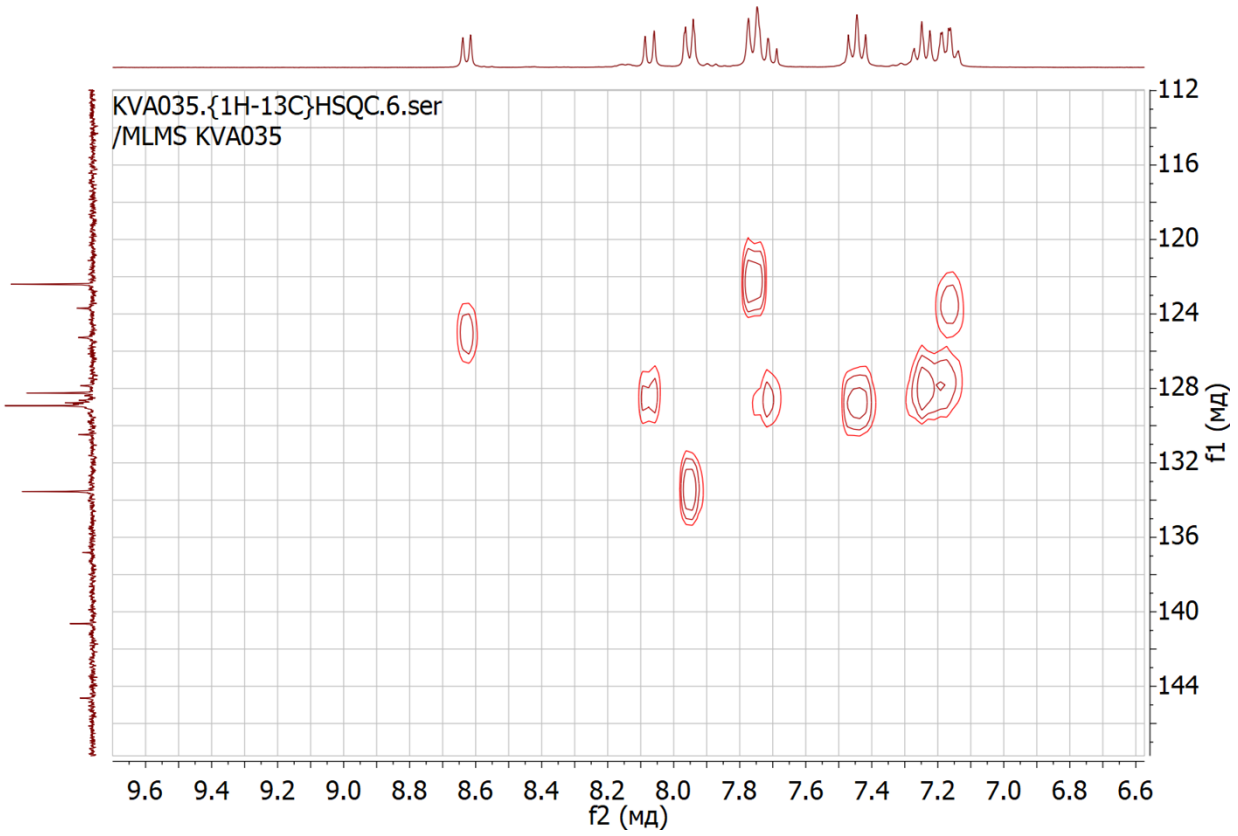
KVA035.{1H-13C}HSQC.6.ser
/MLMS KVA035
112
116
120
124
128
132
136
140
144
f1 (мд)
9.6
9.4
9.2
9.0
8.8
8.6
8.4
8.2
8.0
7.8
7.6
7.4
7.2
7.0
6.8
6.6
f2 (мд)

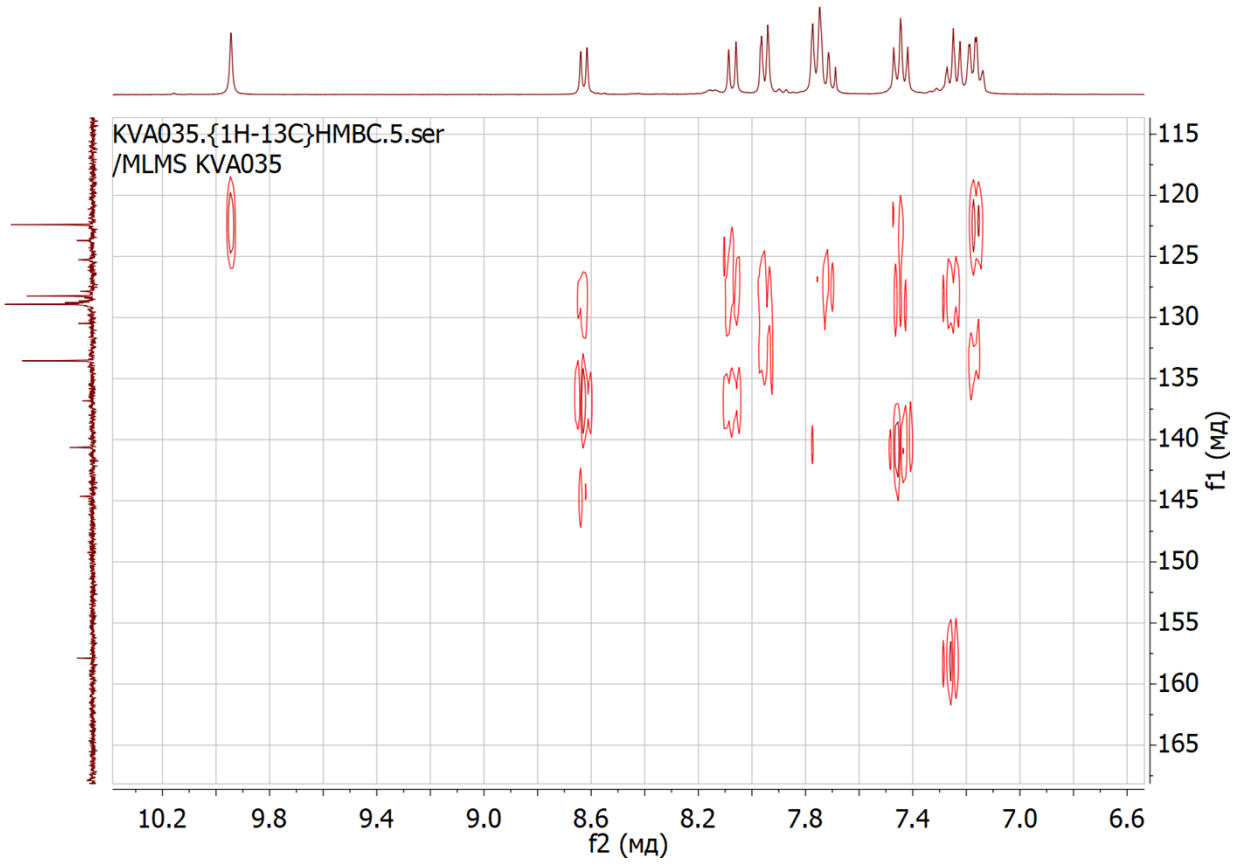
KVA035.{1H-13C}HMBC.5.ser
/MLMS KVA035
115
120
125
130
135
140
145
150
155
160
165
f1 (мд)
10.2
9.8
9.4
9.0
8.6
8.2
7.8
7.4
7.0
6.6
f2 (мд)

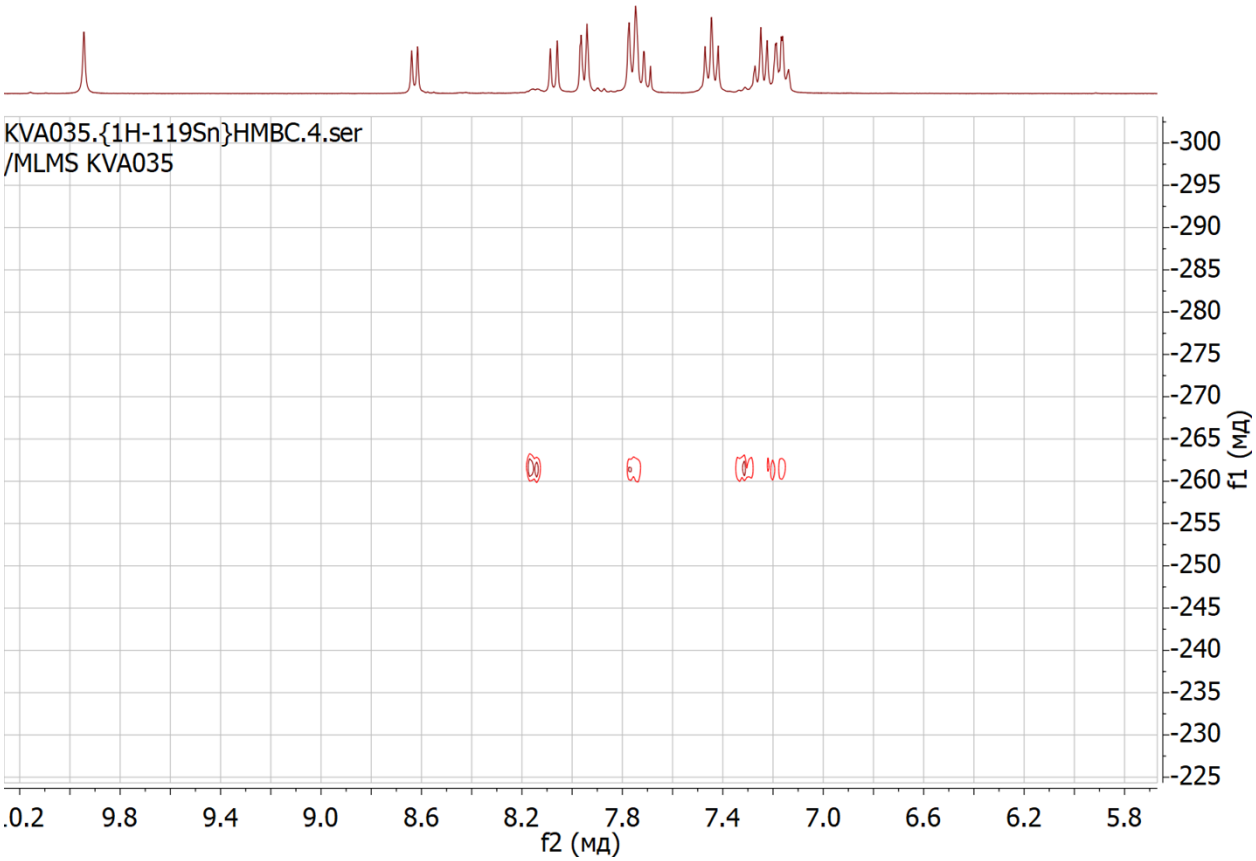

Figure S5. NMR, IR, and mass spectra for **3**.

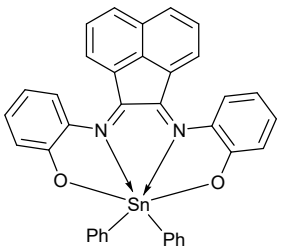
N
N
O
O
Sn
Ph
Ph

4

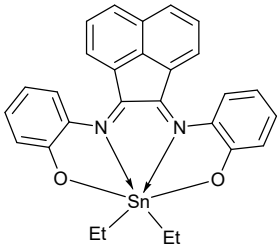
N
N
O
O
Sn
Et
Et

5

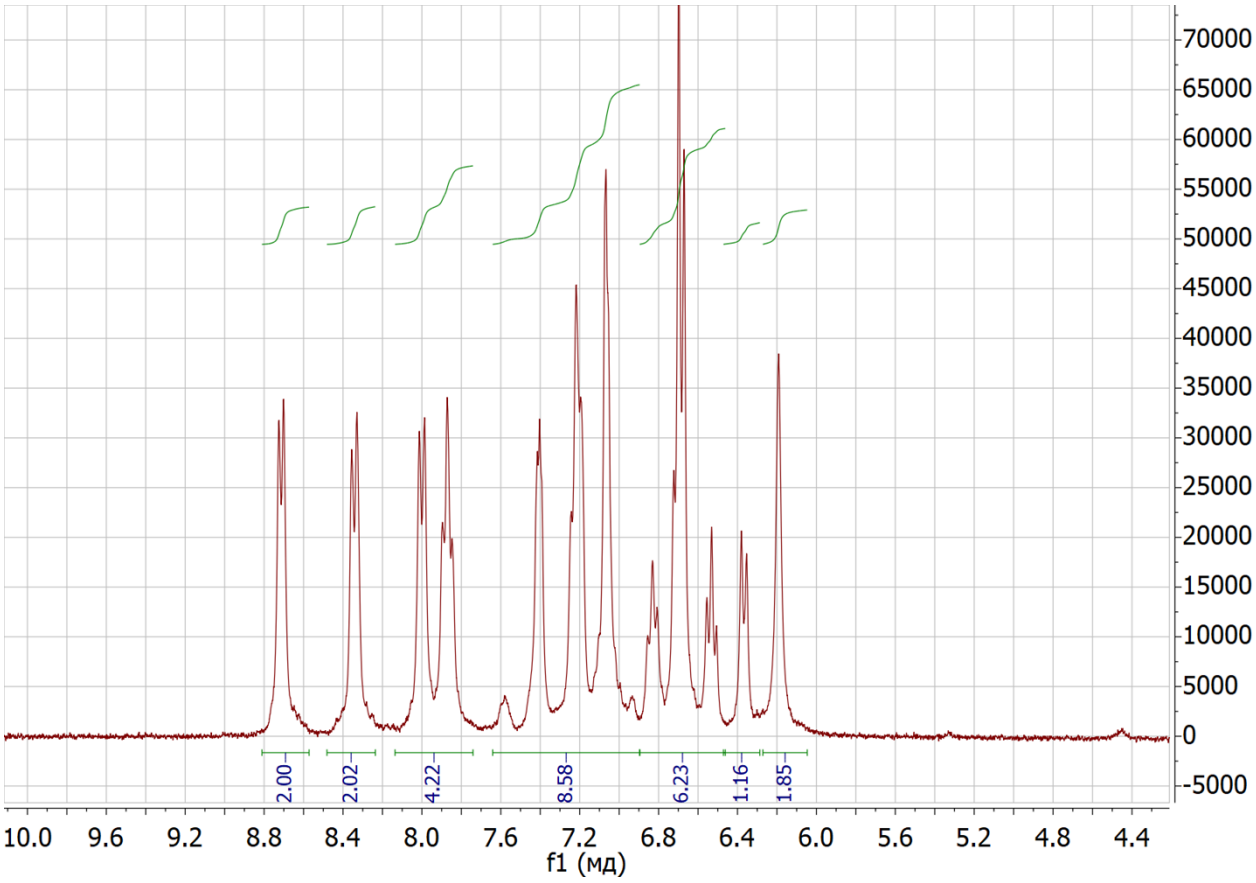
70000
65000
60000
55000
50000
45000
40000
35000
30000
25000
20000
15000
10000
5000
0
-5000
2.00
2.02
4.22
8.58
6.23
1.16
1.85
10.0
9.6
9.2
8.8
8.4
8.0
7.6
7.2
6.8
6.4
6.0
5.6
5.2
4.8
4.4
f1 (мд)

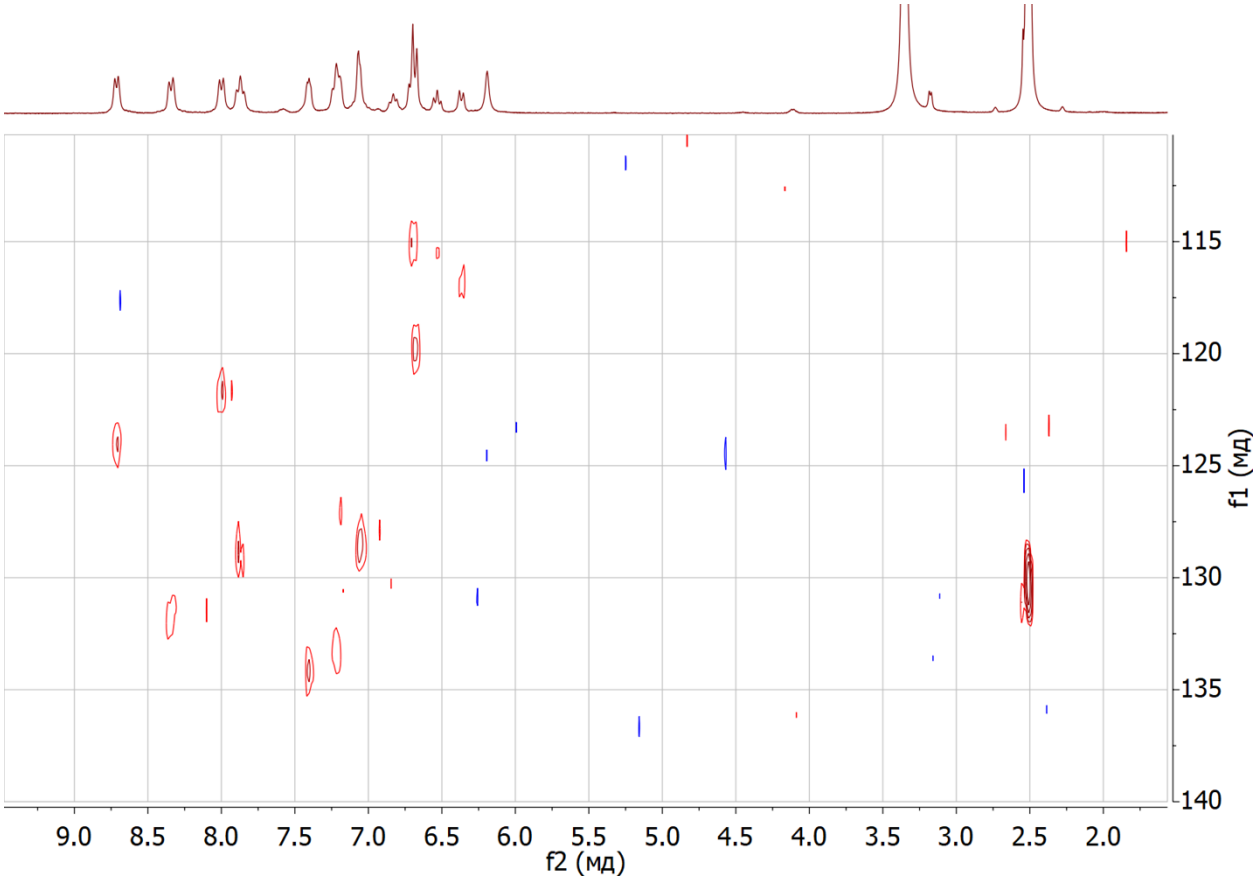

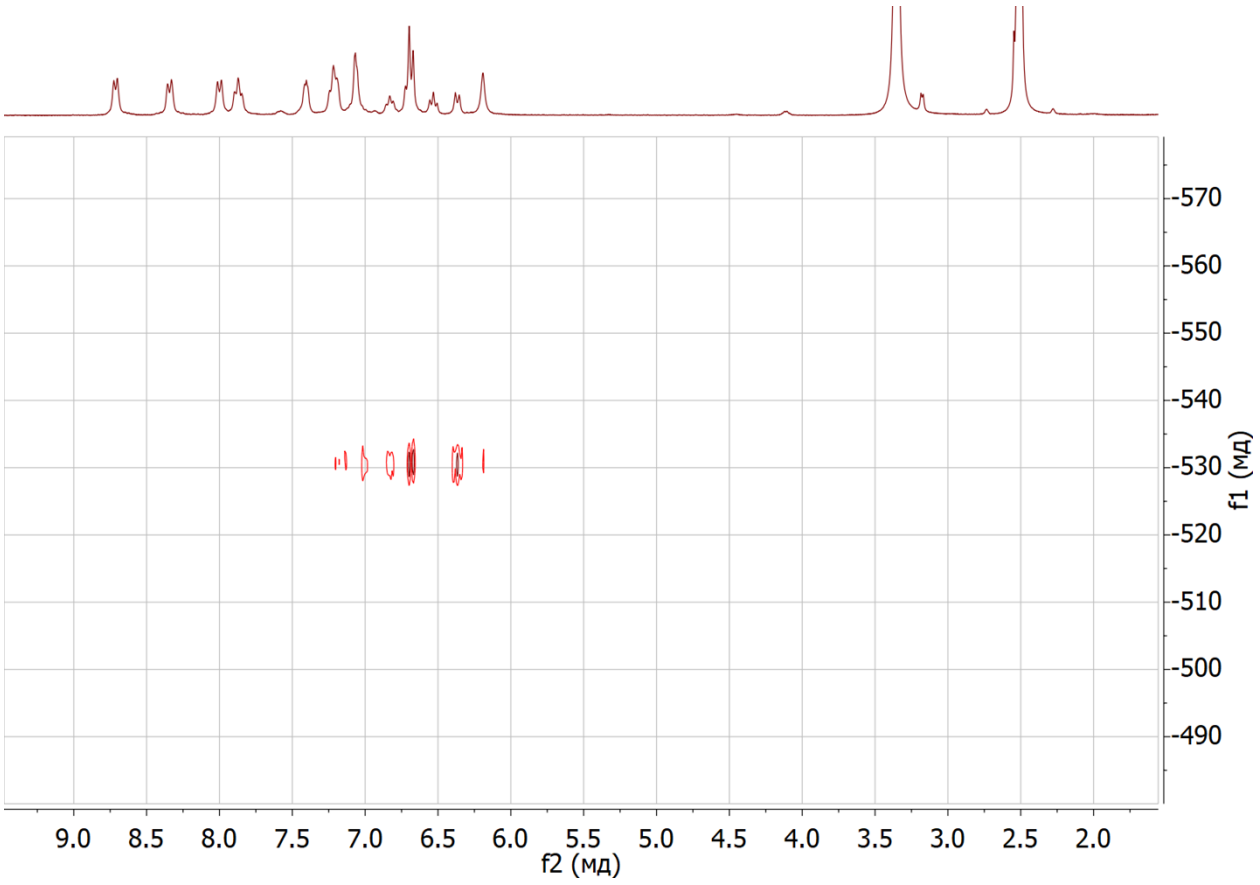

Figure S6. NMR, IR, and mass spectra for complex **4**.

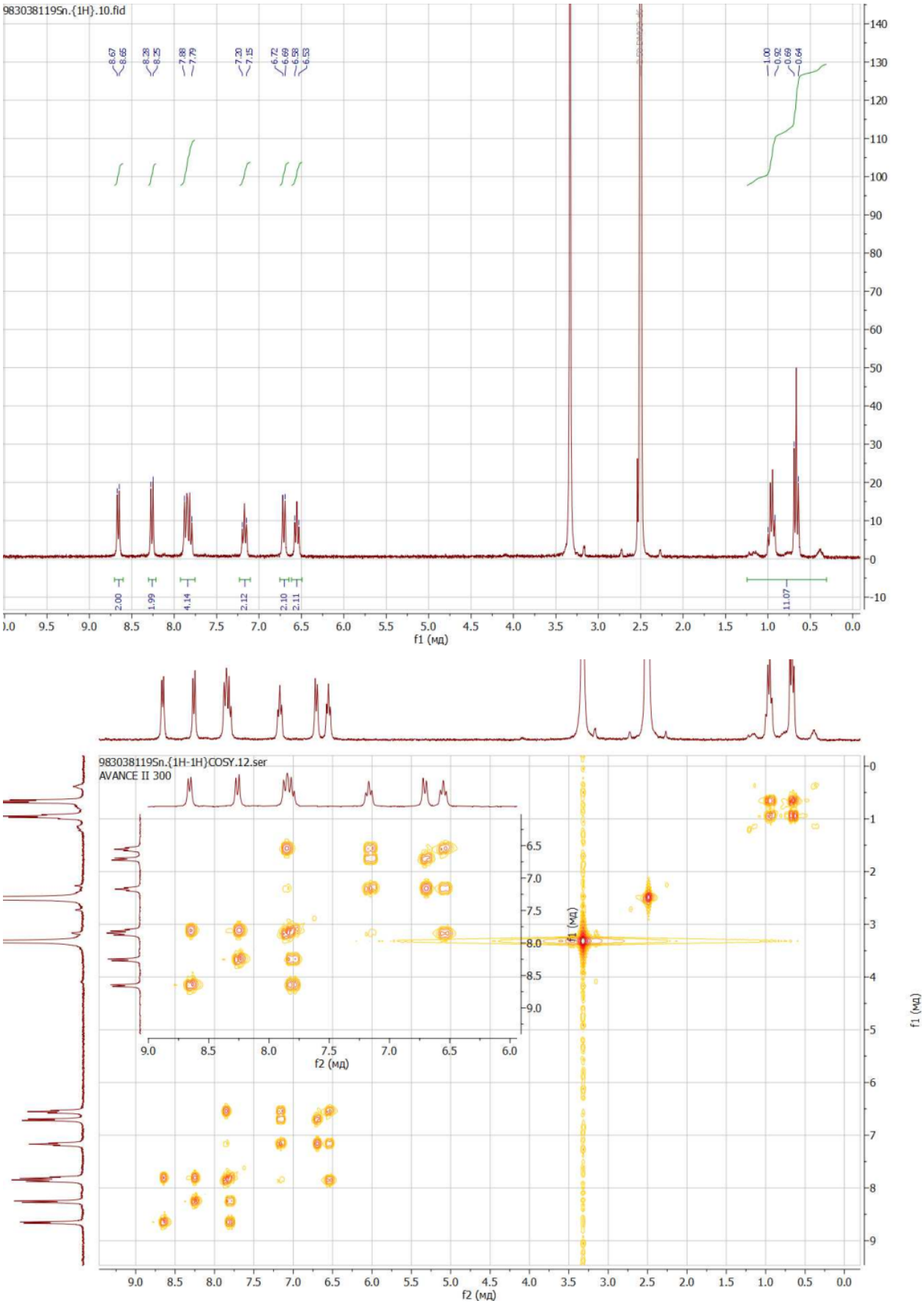
9830381195n.{1H}.10.fid
8.67
8.65
8.28
8.25
7.88
7.79
7.20
7.15
6.72
6.69
6.58
6.53
1.00
0.92
0.69
0.64
2.00
1.99
4.14
2.12
2.10
2.11
11.07
f1 (мд)
9830381195n.{1H-1H}COSY.12.ser
AVANCE II 300
f2 (мд)
f1 (мд)

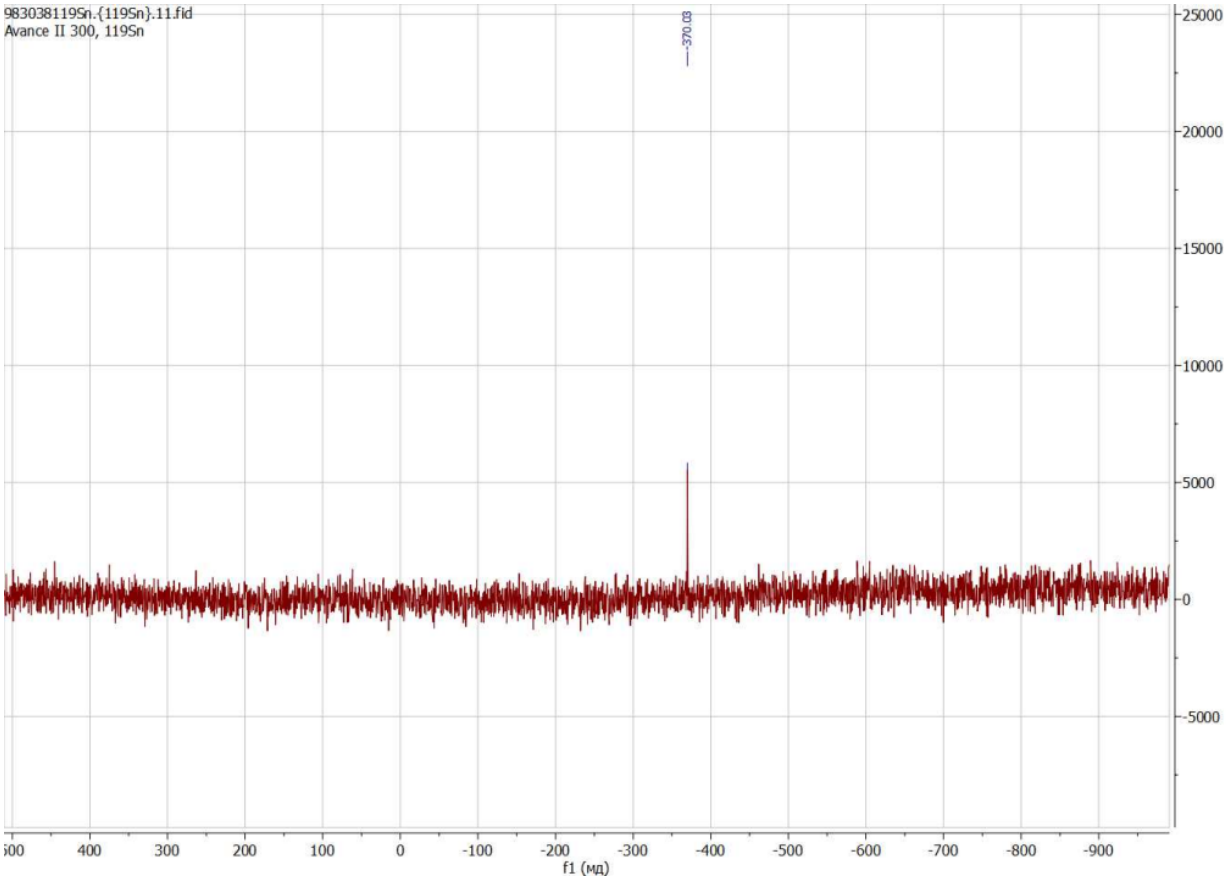
9830381195n.{119Sn}.11.fid
Avance II 300, 119Sn
-370.03
25000
20000
15000
10000
5000
0
-5000
400
300
200
100
0
-100
-200
-300
-400
-500
-600
-700
-800
-900
f1 (мд)

Acquisition Parameter

Source Type	ESI	Ion Polarity	Positive	Set Nebulizer	0.4 Bar
Focus	Not active			Set Dry Heater	180 °C
Scan Begin	50 m/z	Set Capillary	4500 V	Set Dry Gas	4.0 l/min
Scan End	3000 m/z	Set End Plate Offset	-500 V	Set Divert Valve	Waste

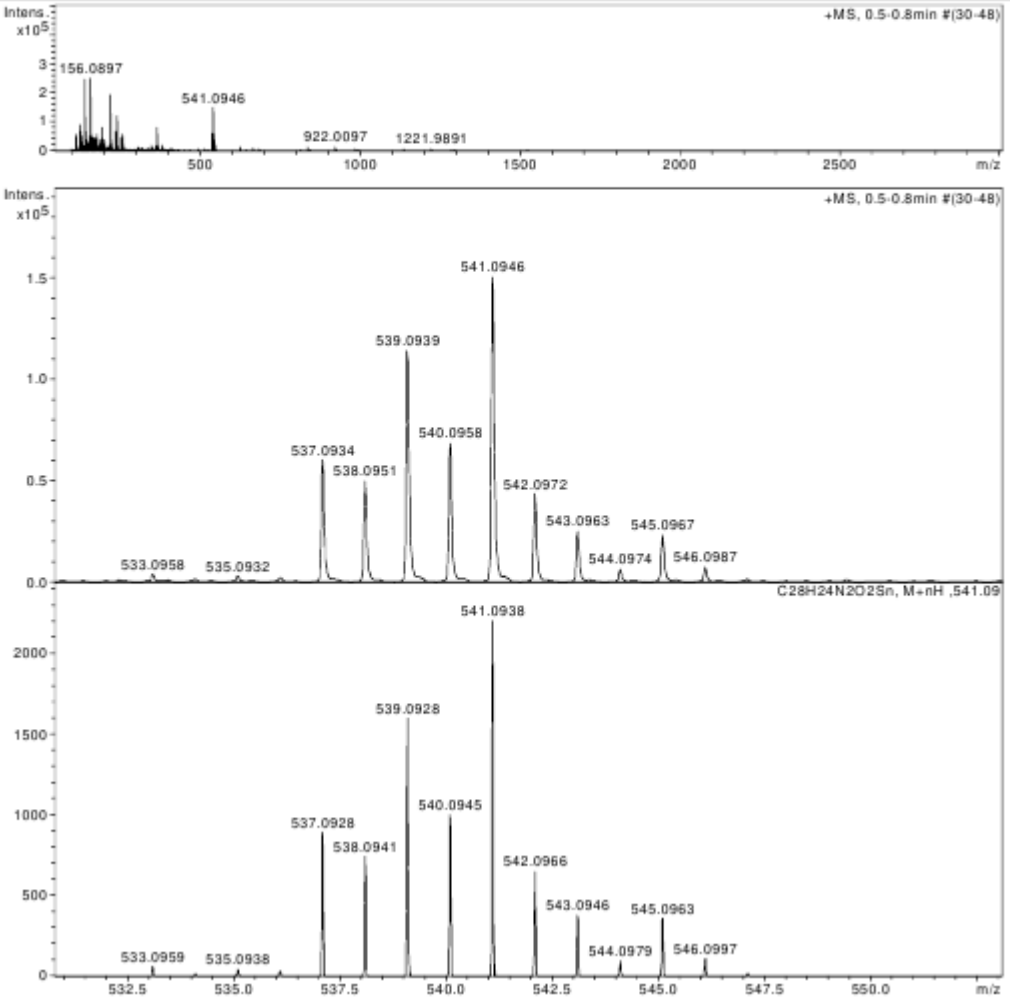

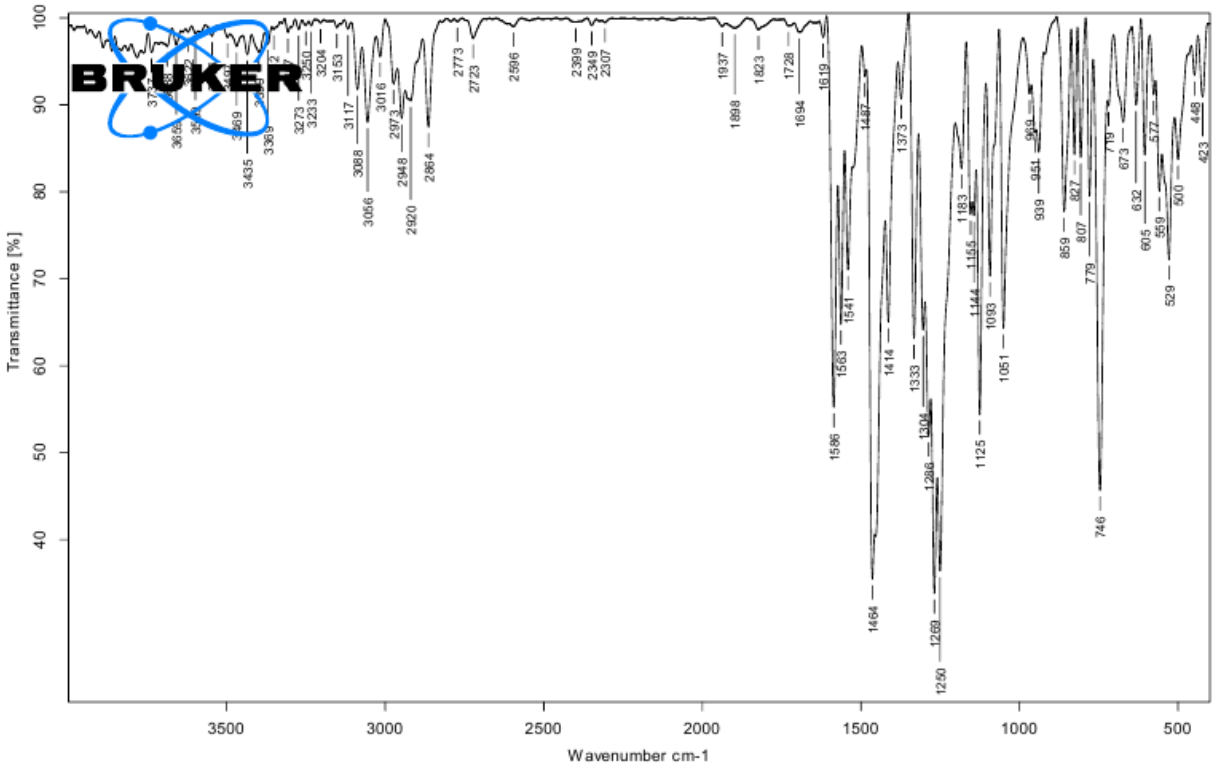

Figure S7. NMR, IR, and mass spectra for complex **5**.

S5. Quantum-chemical calculations

To rationalize the results of experiments performed in solutions, calculations were carried out using the model geometry optimized in a DMF solution at the B3LYP/Def2-TZVP level of theory.[6–7,8] Vibrational frequencies were computed for each optimized geometry in order to verify whether they match the local minimum on PES.[9,10] Energies of electronic transitions and their oscillator strengths in the electronic absorption spectra of **2** were computed via time-dependent DFT[11] at the TD-B3LYP/def2-TZVP level. The solvent (DMF) was taken into account according to the CPCM model.[12] All calculations were performed in the ORCA 4.0.1 software.[13]

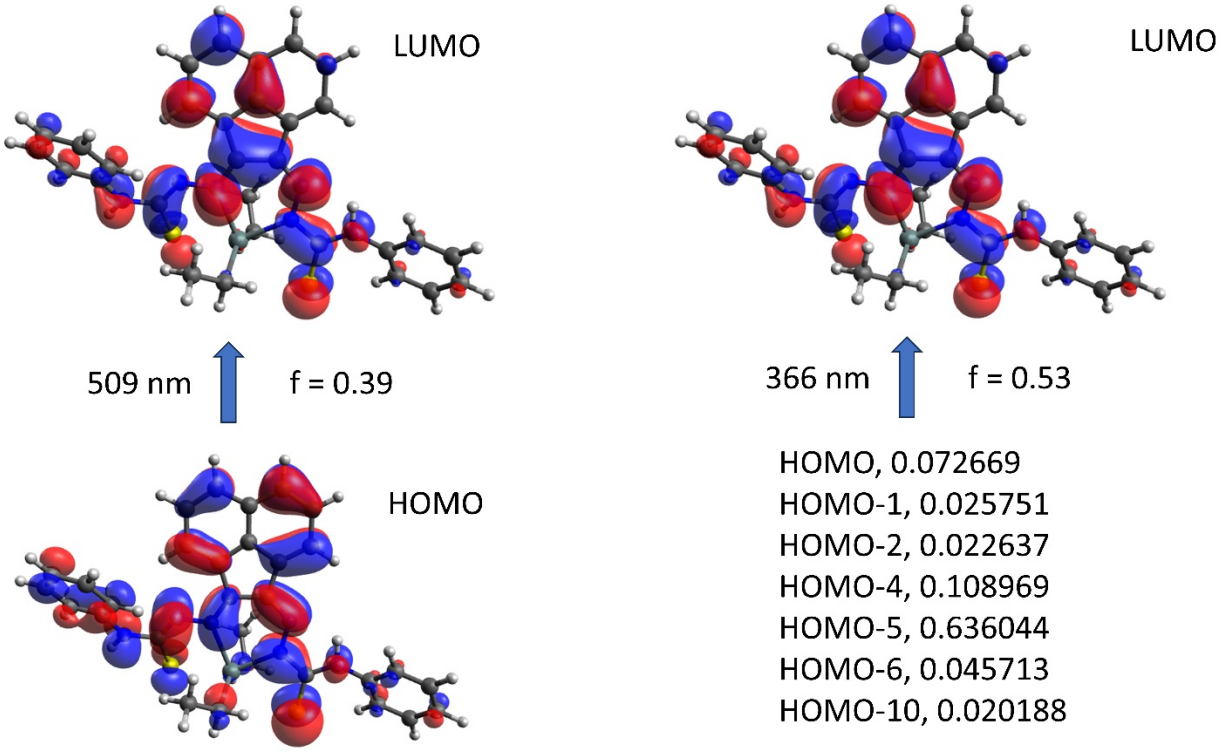

Figure S8. Molecular orbitals involved in the most intensive transitions in the electronic spectrum of complex **2**; for the transition at 366 nm, the weight of the individual excitations are provided if larger than 1.0e-02.

S6. Thermal analysis

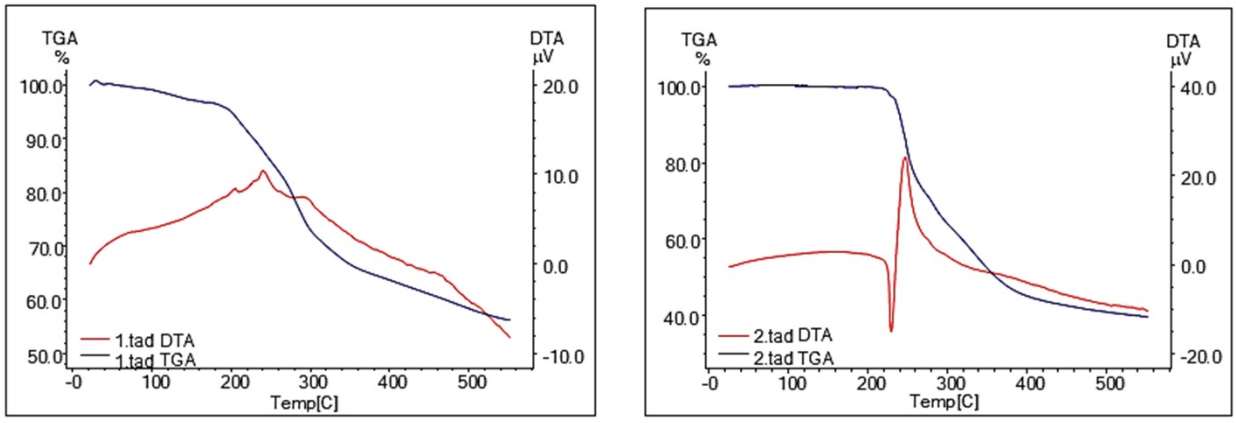

Figure S9. TGA and DTA curves for complexes **1** and **2** obtained at a heating rate of 10 °C min^{-1} in the range from ambient temperature up to 500 °C under argon atmosphere.

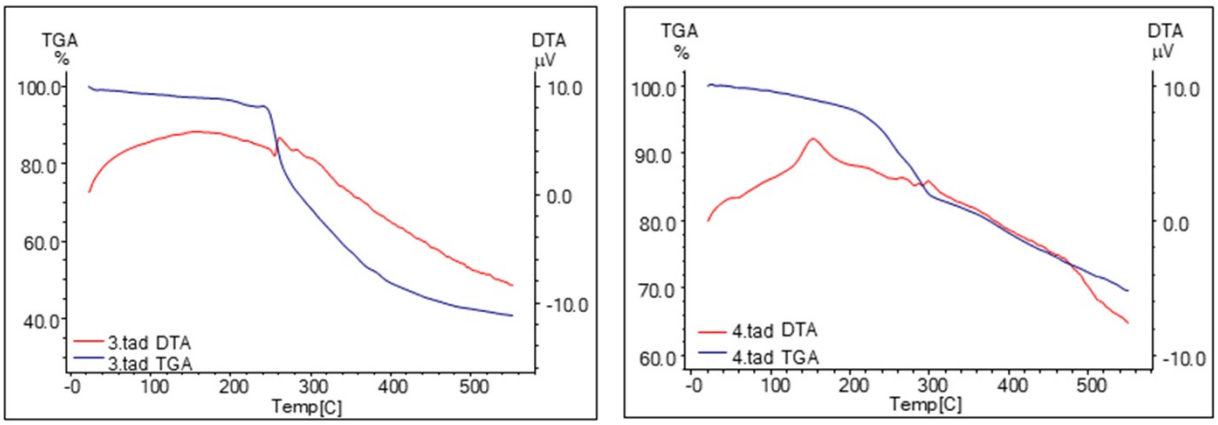

Figure S10. TGA and DTA curves for complexes **3** and **4** obtained at a heating rate of 10 °C min^{-1} in the range from ambient temperature up to 500 °C under argon atmosphere.

References

1 Bruker. APEX-III. Bruker AXS Inc., Madison, Wisconsin, USA, 2019.

2 L. Krause, R. Herbst-Irmer, G. M. Sheldrick and D. Stalke, *J. Appl. Cryst*., 2015, **48**, 3–10, DOI: 10.1107/S1600576714022985.

3 G. M. Sheldrick, *Acta Cryst*., 2015, **A71**, 3–8, DOI: 10.1107/S2053273314026370.

4 G. M. Sheldrick, *Acta Cryst*., 2015, **C71**, 3–8, DOI: 10.1107/S2053229614024218.

5 C. F. Macrae, I. Sovago, S. J. Cottrell, P. T. A. Galek, P. McCabe, E. Pidcock, M. Platings, G. P. Shields, J. S. Stevens, M. Towler and P. A. Wood, *J. Appl. Cryst*. 2020, **53**, 226–235, DOI: 10.1107/S1600576719014092.

6 A. D. Becke, *J. Chem. Phys.*, 1993, **98**, 5648–5652, DOI: 10.1063/1.464913.

7 C. Lee, W. Yang, R. G. Parr, *Phys. Rev. B*, 1988, **37**, 785–789, DOI: 10.1103/physrevb.37.785.

8 F. Weigend and R. Ahlrichs, *Phys. Chem. Chem. Phys.*, 2005, **7**, 3297–3305, DOI: 10.1039/B508541A.

9 H. Jacobsen, A. Bérces, D. P. Swerhone and T. Ziegler, *Comput. Phys. Commun*., 1997, **100**, 263−276, DOI: 10.1016/S0010-4655(96)00119-1.

10 L. Fan and T. Ziegler, *J. Chem. Phys*., 1992, **96**, 9005−9012, DOI: 10.1063/1.462258.

11 A. Dreuw and M. Head-Gordon, *Chem. Rev*., 2005, **105**, 4009–4037, DOI: 10.1021/cr0505627.

12 V. Barone and M. Cossi, *J. Phys. Chem. A,* 1998, **102**, 1995–2001, DOI: 10.1021/jp9716997.

13 F. Neese, *WIREs Comput. Mol. Sci*., 2018, **8**, e1327, DOI: 10.1002/wcms.1327.